AD_____

Award Number: DAMD17-02-1-0344

TITLE: Molecular basis of genomic instability in breast cancer: Regulation of the centrosome duplication cycle

PRINCIPAL INVESTIGATOR: Jian Du, Ph.D.
Gregory Hannon, Ph.D.

CONTRACTING ORGANIZATION: Cold Spring Harbor Laboratory
Cold Spring Harbor, New York 11724

REPORT DATE: June 2004

TYPE OF REPORT: Annual Summary

PREPARED FOR: U.S. Army Medical Research and Materiel Command
Fort Detrick, Maryland 21702-5012

REPORT DOCUMENTATION PAGE

Form Approved
OMB No. 074-0188

1. AGENCY USE ONLY (Leave blank)	2. REPORT DATE	3. REPORT TYPE AND DATES COVERED
	June 2004	Annual Summary (1 Jun 03 - 31 May 04)

4. TITLE AND SUBTITLE
Molecular basis of genomic instability in breast cancer: Regulation of the centrosome duplication cycle

5. FUNDING NUMBERS
DAMD17-02-1-0344

6. AUTHOR(S)
Jian Du, Ph.D.
Gregory Hannon, Ph.D.

7. PERFORMING ORGANIZATION NAME(S) AND ADDRESS(ES)
Cold Spring Harbor Laboratory
Cold Spring Harbor, New York 11724

E-Mail:
duj@cshl.org

8. PERFORMING ORGANIZATION REPORT NUMBER

9. SPONSORING / MONITORING AGENCY NAME(S) AND ADDRESS(ES)
U.S. Army Medical Research and Materiel Command
Fort Detrick, Maryland 21702-5012

10. SPONSORING / MONITORING AGENCY REPORT NUMBER

11. SUPPLEMENTARY NOTES
Report contains color

12a. DISTRIBUTION / AVAILABILITY STATEMENT
Approved for Public Release; Distribution Unlimited

12b. DISTRIBUTION CODE

13. Abstract *(Maximum 200 Words)* *(abstract should contain no proprietary or confidential information)*

Alterations in the expression and activity of the centrosomal kinase, Aurora-A/STK15, affect genomic stability, disrupt the fidelity of centrosome duplication, and induce cellular transformation. In 2003, we finished task 1 and 2. From June 1, 2003 to May 31, 2004, we further charcterized a mitotic spindle-associated protein, astrin/DEEPEST, which is identified as an Aurora-A interacting protein by a two-hybrid screen. Astrin is co-expressed with Aurora-A at mitosis and colocalizes to the mitotic spindles, as well as to the outer kinetochore. RNAi depletion of astrin abolishes the Aurora-A mitotic spindle localization. Depletion of astrin, which interacts with alpha-tubulin, also induces Eg5 depedent multipolar spindle from de novo synthesized centrosomes without recruiting centrin2 protein. Astrin silencing leads to a moderate G2/M cell cycle delay, caused by de=localization of cyclinB1-CDK1 from the centrosome and spindles, which resembles the G2/M arrest phenotypes in siAurora-treated cells. Double-inactivation of both astrin and Aurora-A shows mitotic arrest phenotypes similiar to depletion of siAurora-A alone, suggesting that astrin acts upstream of Aurora-A/ Overexpression of astrin caused premature senescence in primary human fibroblast by inducing p53 overexpression.

14. SUBJECT TERMS
breast cancer biology, genomic instability, aurora-A/STK15, centrosome

15. NUMBER OF PAGES
28

16. PRICE CODE

17. SECURITY CLASSIFICATION OF REPORT	18. SECURITY CLASSIFICATION OF THIS PAGE	19. SECURITY CLASSIFICATION OF ABSTRACT	20. LIMITATION OF ABSTRACT
Unclassified	Unclassified	Unclassified	Unlimited

Table of Contents

Cover.....

SF 298.....

Introduction.....1

Body.....2

Key Research Accomplishments.....5

Reportable Outcomes.....5

Conclusions.....5

References.....5

Appendices.....9

Introduction

The eukaryotic centrosome is the microtubule organizing center and is composed of two perpendicularly positioned centrioles and surrounding amorphous pericentriolar materials (reviews (Zheng, Jung et al. 1991), (Hinchcliffe and Sluder 2001), (Bornens 2002) (Rieder, Faruki et al. 2001) (Doxsey 2001) (Stearns 2001)). Four groups of protein kinases are found to associate with and regulate the centrosome replication cycle: cyclin-dependent kinases (Hinchcliffe, Li et al. 1999) (Matsumoto, Hayashi et al. 1999) (Meraldi, Lukas et al. 1999); Polo-like kinases (do Carmo Avides, Tavarest et al. 2001); NIMA kinases (Fry 2002); and Aurora kinases. In mammalian cells, the Aurora kinase family has three members: Aurora-A, -B, and –C. Alterations in the expression and activity of Aurora-A/STK15 affect genomic stability, disrupt the fidelity of centrosome duplication, and induce cellular transformation (Zhou, Kuang et al. 1998) (Tanaka, Kimura et al. 1999) (Miyoshi, Iwao et al. 2001) (Sen, Zhou et al. 2002). Aurora-A is regulated on protein expression level by ubiquitin pathways and protein modifications, such as phosphorylation (Farruggio, Townsley et al. 1999) (Walter, Seghezzi et al. 2000) (Honda, Mihara et al. 2000) (Katayama, Zhou et al. 2001), as well as by interacting partners, such as TPX2 (Kufer, Silljé et al. 2002) (Garrett, Auer et al. 2002) (Tsai, Wiese et al. 2003). Eg5 (a kinesin related protein), CPEB (cytoplasmique polyadenylation element binding protein), and TACC3 (Transforming acidic coiled coil protein number 3) have been found to be substrates of Aurora-A (Giet, Uzbekov et al. 1999) (Mendez, Hake et al. 2000) (Groisman, Huang et al. 2000) (Giet, McLean et al. 2002).

Microtubules are composed of heterodimers of α– and β-tubulins. The mitotic spindle, composed primarily of microtubules and associated proteins, is responsible for attaching to the condensed sister chromatids at the kinetochore and accurately segregating them to two daughter cells (Compton 2000). Microtubule-associated proteins have two groups: motor proteins and nonmotor proteins. Motor proteins participate in microtubule sliding, chromosomes movement along spindle microtubules, and microtubule assembly dynamics. These include cytoplasmic dynein/dynactin and the kinesin family proteins (e.g. Kar3/NCD proteins), which are minus end directed motors (Verde, Berrez et al. 1991) (Heald 2000) (Sharp, Rogers et al. 2000) (Mountain V 1999) (Endow, Kang et al. 1994), and kinesin-like protein Eg5, which is a plus end-directed protein (Wilson, Fuller et al. 1997) (Blangy, Lane et al. 1995). Non-motor proteins include microtubule-stabilizing factors that work by increasing microtubule growth rate, including XMAP230 and related proteins (Andersen, Buendia et al. 1994) (Charrasse, Schroeder et al. 1998), and microtubule-destabilizing factors and facilitate the disassembly of microtubules, such as OP18/Stathmin and katanin (Belmont and Mitchison 1996) (McNally, Okawa et al. 1996). Other structural proteins, like NuMA, TPX2, TACC, and Orbit (Compton and Cleveland 1994) (Merdes A 1996) (Wittmann, Wilm et al. 2000) (Gergely, Karlsson et al. 2000) (Inoue, do armo Avides et al. 2000), may act as scaffolds in centrosome and spindle dynamics.

We followed the proposal task 1 to 4 to finish the purification of the Aurora-A protein complex, characterize one of Aurora-A substrate, p160ROCK, which can work

together with Aurora-A kinase to promote the genomic instability in breast and other cancer cell lines (The results are published in PNAS (2004), see appendices). During the past 12 months (June 1, 2003 to May 31, 2004), we further characterized an Aurora-A interacting protein, astrin, which is an upstream regulator of Aurora-A localization at mitotic spindles and overexpression leads to p53-dependent cellular senescence.

Body

Human astrin/DEEPEST was identified as a mitotic spindle-associated non-motor protein that localized to spindle microtubules from prophase through anaphase (Chang, Huang et al. 2001) (Mack and Compton 2001) (Gruber, Harborth et al. 2002). Astrin is a 134 kDa protein with two coiled-coil domains at the C-terminus. Silencing of astrin in HeLa cells by RNA interference resulted in a growth arrest, multipolar formation and highly disordered spindles (Gruber, Harborth et al. 2002). In the absence of astrin, condensed chromosomes could not align to the spindle equator, ultimately leading to apoptosis (Gruber, Harborth et al. 2002). Astrin was found to be phosphorylated by p34cdc2 kinase in vitro (Chang, Huang et al. 2001). (Chang, Chen et al. 2003)

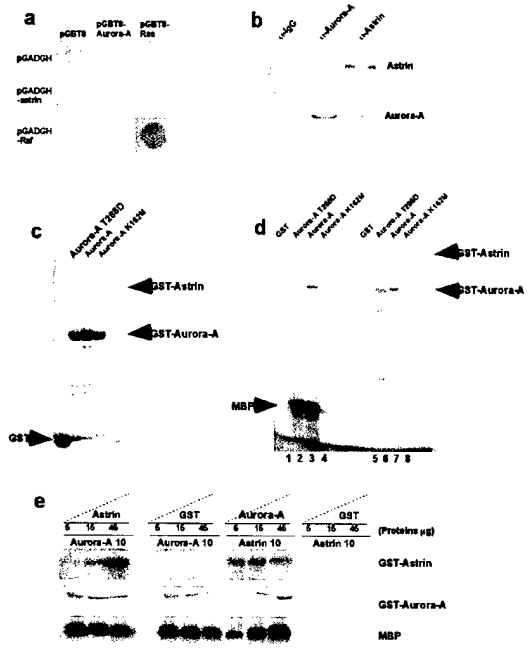

Figure 1 Astrin and Aurora-A interact. (a) Transformants of *S. cerevisiae* pJ64-4a were patched on synthetic complete plates selected for both pGBT and pGADGH derivatives. The patches were transformed to Whatman No.1 paper for β-galactosidase assay with X-gal as substrate. The assay were developed at 37°C for 1 hour. (b) Hela cell lysates were immunoprecipitated with anti-IgG (negative control), -astrin or –Aurora-A, respectively. The immunoprecipitates were applied to western blot. (c) E. coli BL21 expressed GST-astrin and –Aurora-A fusion proteins were purified with glutathione-agarose beads and fractionated on SDS-PAGE. (d) Kinase assays using 10 μg each of GST-astrin, –Aurora-As (wild type, constitutively active T288D, and kinase-dead K162M mutations) and MBP as a substrate at 37°C for 15 min. The reactions were resolved on SDS-PAGE and subjected to autoradiography. Phosphorylated astrin and autophosphorylated Aurora-A are indicated on the right. (e) Kinase assays with increased amount of GST (control), GST-astrin or –Aurora-A were done as in (d). It did not show that astrin regulates autophosphorylation of Aurora-A.

Astrin/DEEPEST was identified as an Aurora-A interacting protein by a two- hybrid screen (Fig.1). Astrin co-immunoprecipitated with Aurora-A *in vivo* and can be phosphorylated by it *in vitro* (Fig.1). Astrin is co-expressed with Aurora-A at mitosis and colocalizes to the mitotic spindles, as well as to the outer kinetochore (Fig.2). RNAi depletion of astrin abolishes the Aurora-A mitotic spindle localization (Fig.3). Depletion of astrin, which interacts with α-tubulin, also induces Eg5 dependent multipolar spindles from *de novo* synthesized centrosomes without recruiting centrin2 protein (Fig.4-5). Astrin silencing leads to a moderate G2/M cell cycle delay, caused by de-localization of cyclin B1-CDK1 from the centrosomes and spindles, which resembles the G2/M arrest phenotypes in siAurora-A treated cells (Fig.4). Double-inactivation of both astrin and Aurora-A shows mitotic arrest phenotypes similar to depletion of siAurora-A alone, suggesting that astrin acts upstream of Aurora-A. Overexpression of astrin caused premature senescence in primary human fibroblast cells by inducing p53 overexpression (Fig.6). The work partially fulfilled the task 4, which includes further

further purification and characterization of Aurora-A/STK15 substrates, albeit from a different screen. The work is summarized in the recent manuscript ready for submission

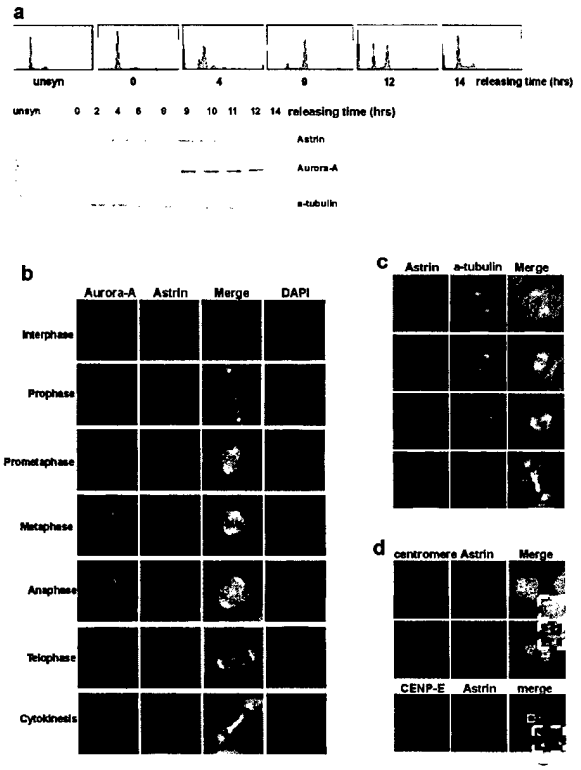

Figure 2. Astrin and Aurora-A co-expressed and colocalized at mitosis (a) Hel cells were synchronized at S-phase and released into next cell cycle. Cells at various time-points were collected and analyzed by flow cytometry immunoblot. "Unsys" indicates the unsynchronized cells. Numbers indicate the time from the releasing point. Proteins are labeled at right. (b) (c) (d) Hela cells on cover slips were fixed and stained for immunofluorescence by anti-astrin, -Aurora-A, α-tubulin, -CREST, or CENP-E, and DAPI. Inserts in (d) represent the higher-amplification of kinetochore stains. Arrows indicate the significant overlap of anti-astrin with -CENP-E stains.

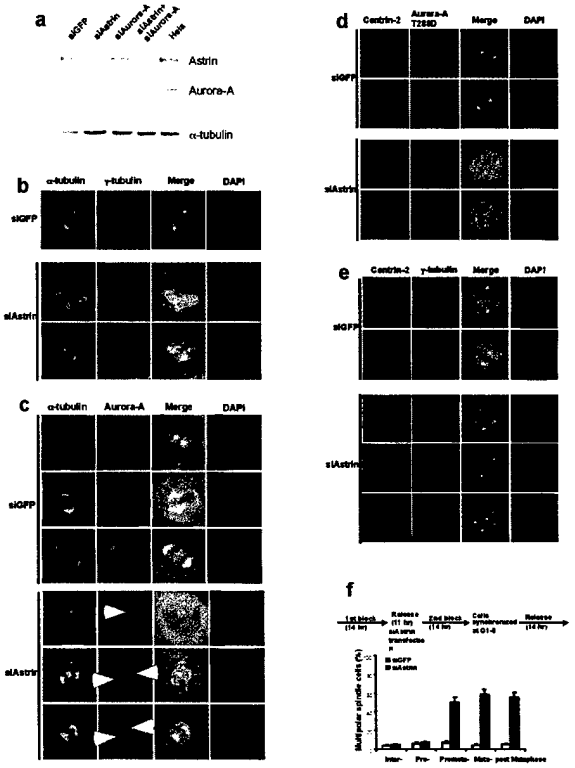

Figure 3. Depletion of astrin delocalized Aurora-A from induced multipolar spindles (a) Hela cells transfected with siGFP (control), siAstrin, siAurora-A, or both were lysed and subjected to immunoblot analysis. Proteins are indicated on the right. (b), (c), (d), (e) HeLa cells seeded on cover slips were transfected with siRNAs and fixed for immunofluorescence with anti-tubulin, -Aurora-A, -Aurora-A288D specific, -centrin 2, -γ-tubulin, and DAPI. (f) siAstrin transfection was incorporated after the first HeLa cell cycle block. Synchronized cells released into next cycle were collected at different time-points and subjected to immunostaining with anti-centrin 2 and -γ-tubulin. Cells carrying multiple (>2) γ-tubulin spots were counted and plotted. More than 300 interphase and 300 mitotic cells were counted.

The work from the past year together with that of 2003 fulfilled the tasks 1, 2 and partially 4. For Task 3: Construct and validate the chemical genetic methods for STK15, we constructed the STK15 mutations collaborating with Dr. K. Shokat. The purified mutant stk15L210A/L210G abolished the kinase activity on natural ATP (data not shown). However, selecting the ATP analogs turned out not to be a trivial experiment (Specht and Shokat 2002) and we did not have much success on it. Since we have several interesting candidates from the purification of Aurora-A complex, we will concentrate on these components for further characterization.

For Task 5-6: Construction of cDNA libraries from breast cancer cell lines and a genetic screen for centrosome abnormalities in Rat1 or 3T3/GFP-cen2 cells, a more powerful screen approach for genes involved in genetic instability in breast cancer is merging (Hannon 2002). We will approach the RNAi screen with the human genome-wide shRNA library constructed in the lab to look for suppressors of Aurora-A

knockdown, which renders a mitotic arrest and eventually apoptosis in Hela cells.

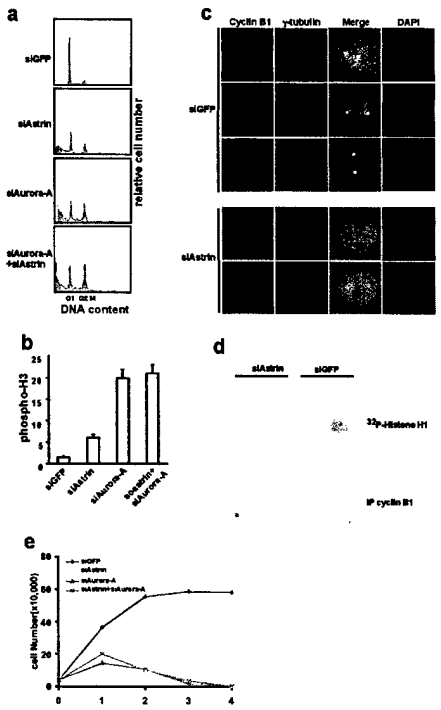

Figure 4. Depletion of astrin caused G2/M delay. (a) Hela cells transfected with various siRNAs were collected and fixed for flow cytometry analysis. (b) cells in (a) were stained with anti-phospho-H3 immunofluorescence. (c) Cells in (a) were stained with anti-Cyclin B1 and γ-tubulin immunofluorescence. (d) Cell extracts from siGFP (control) and siAstrin treated cells were immunoprecipitated with anti-Cyclin B1 antibody. The resulting precipitates were subjected both for CDK1 kinase assay using histone h1 as substrate, and for immunoblot with anti-cyclin B1 antibody. (e) Hela cells were seeded into 35 mm plates and transfected with siRNAs. At the indicated time (days), cells were collected, cell numbers counted, and plotted.

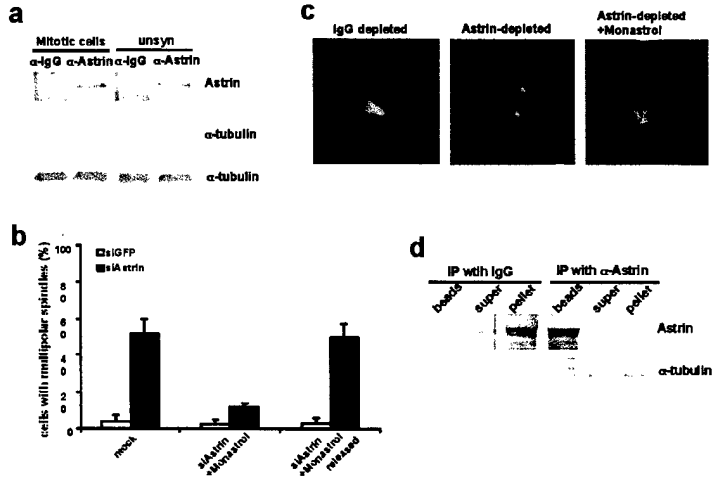

Figure 5. Astrin interacts with tubulins (a) HeLa cell lysates from unsynchronized or mitotic arrested cells were immunoprecipitated with anti-IgG (negative control), or anti-Astrin antibody (lanes 1 and 2 rows). The immunoprecipitates were subjected to immunoblot analysis. Proteins are indicated on the right. The lysates were also analyzed by immunoblot with anti-tubulin (lower row) to insure that immunoprecipitations were processed from the same amount of initial materials. (b) Hela cells transfected with siGFP (negative control) or siAstrin were treated with monastrol (siAstrin+Monastrol) or DMSO (mock lanes) for 5 hours. The cells were fixed for anti-γ-tubulin immunofluorescence to access the cells carrying multiple centrosomes. Samples released from monastrol inhibition for another 1 hour (siAstrin+Monastrol released) were also processed for similar immunostaining. (c) Microtubule organization from anti-IgG (negative control, rabbit IgG panel), astrin depleted (astrin-depleted panel), or astrin-depleted together with 100 uM monastrol (astrin-depleted+monastrol panel). Hela cell mitotic extracts were examined by anti-tubulin immunoblotting. Proteins associated with immunoprecipitated beads (beads), and the resulting supernatants (super) and aster-precipitated pellet (pellet) from IgG- and astrin-depleted were analyzed by immunoblot. Proteins are labeled on the right.

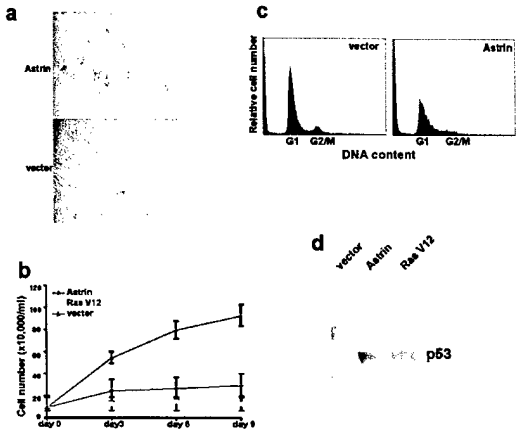

Figure 6. Astrin overexpression induced primary IMR90 cell senescence. (a) human IMR90 cells were infected with pMaopuro (vector alone), pMaopuro, or RasV12-pMaopuro retrovirus and selected with puromycin for 3 days. Cells were stained with X-gal for overnight at 37°C 6 days post selection. (b) The puromycin resistant cells were plated out at 10,000 cells/ml onto 60 mm plates. At the indicated time-points, cells were collected, counted and plotted. 3 experiments were repeated and standard errors are indicated. (c) Cells as in (a) were analyzed by flow cytometry. (d) Cell extracts from (a) were collected and immunoblotted with anti-p53.

Research Accomplishment:

- Immunoprecipitated and purified the STK15-associate-factor complex (SAF) and characterized a STK15 kinase substrate *in vivo*, p160ROCK (Jian Du, Gregory J. Hannon (2004). Suppression of p160ROCK bypass cell cycle arrest following Aurora-A/STK15 depletion. *Proceeding of National Academy of Sciences*, 101:8975-8980).

- In a 2-hybrid screen looking for STK15 interacting proteins (may also identify its substrates) using full length STK15 as a bait, we isolated and characterized the mitotic spindle-associated Astrin, which regulates the Aurora-A mitotic spindle localization (Jian Du, Sandra Jablonski, Tim Yen, and Gregory J. Hannon. Depletion of astrin delocalizes Aurora-A/STK15 on induced multipolar spindles, In preparation)

- On-going RNAi genetic screen for suppressors of Aurora-A knockdown, which leads mitotic arrest and eventually apoptosis in Hela cells, using the genome-wide shRNA library constructed in the lab.

Reportable Outcomes:

(1) Jian Du, Gregory J. Hannon (2002). The centrosomal kinase Aurora-A/STK15 interacts with a putative tumor suppressor NM23-H1. *Nuclei Acid Research*, 30: 5465-5475

(2) Jian Du, Gregory J. Hannon (2004). Suppression of p160ROCK bypass cell cycle arrest following Aurora-A/STK15 depletion. *Proceeding of National Academy of Sciences*, 101:8975-8980

(3) Jian Du, Sandra Jablonski, Tim Yen, and Gregory J. Hannon. Depletion of astrin delocalizes Aurora-A/STK15 on induced multipolar spindles, In preparation

Conclusion:

We fulfilled Task 1, 2 and partially 4. Task 3 is changed now because of technical difficulty. Task 5 and 6 with revision are under investigation.

References:

Andersen, S. S., B. Buendia, et al. (1994). "Effect on microtubule dynamics of XMAP230, a microtubule-associated protein present in Xenopus laevis eggs and dividing cells." J. Cell Biol. **27**: 1289–1299.

Belmont, L. and T. J. Mitchison (1996). "Identification of a protein that interacts with tubulin dimers and increases the catastrophe rate of microtubules." Cell **84**: 623-631.

Blangy, A., H. A. Lane, et al. (1995). "Phosphorylation by p34cdc2 regulates spindle association of human Eg5, a kinesin-related motor essential for bipolar spindle formation in vivo." Cell **87**: 1159-1169.

Bornens, M. (2002). "Centrosome composition and microtubule anchoring mechanisms." Curr Opin Cell Biol. **14**: 25-34.

Chang, M. S., C. Y. Chen, et al. (2003). "Expression and promoter analysis of mouse mastrin gene." Biochem. Biophys. Res. Commun. **307**: 491-497.

Chang, M. S., C. J. Huang, et al. (2001). "Cloning and characterization of hMAP126, a newmembe r of mitotic spindle-associated proteins,." Biochem. Biophys. Res. Commun. **287**: 116-121.

Charrasse, S. M., M. Schroeder, et al. (1998). "The TOGp protein is a new human microtubule-associated protein homologous to the Xenopus XMAP215." J. Cell Biol. **111**: 1371-1383.

Compton, D. A. (2000). "Spindle assembly in animal cells." Annu. Rev. Biochem. **69**: 95-114.

Compton, D. A. and D. W. Cleveland (1994). "NuMA, a nuclear protein involved in mitosis and nuclear reformation." Curr. Opin. Cell Biol. **6**: 343-346.

do Carmo Avides, M., A. Tavarest, et al. (2001). "Polo kinase and Asp are needed to promote the mitotic organizing activity of centrosome." Nature Cell Biol. **3**: 421-424.

Doxsey, S. (2001). "Re-evaluating centrosome function." Nature Rev. Mol. Cel.l Biol. **2**: 688-98.

Endow, S. A., S. J. Kang, et al. (1994). "Yeast Kar3 is a minus-end microtubule motor protein that destabilizes microtubules preferentially at the minus ends." EMBO J. **13**: 2708-2713.

Farruggio, D. C., F. M. Townsley, et al. (1999). "Cdc20 associates with the kinase aurora2/Aik." Proc. natl. Acad. Sci. USA **96**: 7306-7311.

Fry, A. M. (2002). "The Nek2 protein kinase: a novel regulator of centrosome structure." Oncogene **21**: 6184-6194.

Garrett, G., K. Auer, et al. (2002). "hTPX2 Is Required for Normal Spindle Morphology and Centrosome Integrity during Vertebrate Cell Division." Curr. Biol. **12**: 2055-2059.

Gergely, F., C. Karlsson, et al. (2000). "The TACC domain identifies a family of centrosomal proteins that can interact with microtubules." Proc. Natl. Acad. Sci. USA **97**: 14352-14357.

Giet, R., D. McLean, et al. (2002). "Drosophila Aurora A kinase is required to localize D-TACC to centrosomes and to regulate astral microtubules." J. Cell. Biol. **156**: 437-451.

Giet, R., R. Uzbekov, et al. (1999). "The Xenopus laevis centrosome aurora/Ipl1-related kinase." Biol. Cell **91**: 461-470.

Groisman, I., Y. S. Huang, et al. (2000). "CPEB, maskin, and cyclin B1 mRNA at the mitotic apparatus: implications for local translational control of cell division." Cell **103**: 435-447.

Gruber, J., J. Harborth, et al. (2002). "The mitotic-spindle associated protein astrin is essential for progression through mitosis,." J. Cell Sci. **115**: 4053-4059.

Hannon, G. J. (2002). "RNA interference." Nature **418**: 244-251.

Heald, R. (2000). "Motor function in the mitotic spindle." Cell **102**: 399-402.

Hinchcliffe, E. H., C. Li, et al. (1999). "Requirment of Cdk2-cyclin E activity for repeated centrosome reproduction in *Xenopus* egg extracts." Science **283**: 851-854.

Hinchcliffe, E. H. and G. Sluder (2001). "Centrosome duplication: three kinases come up a winner!" Curr Biol. **11**: R698-701.

Honda, K., H. Mihara, et al. (2000). "Degradation of human Aurora2 protein kinase by the anaphase-promoting complex-ubiquitin-proteasome pathway." Oncogene **19**: 2812-2819.

Inoue, Y. H., M. do armo Avides, et al. (2000). "Orbit, a novel microtubule-associated protein essential for mitosis in Drosophila melanogaster,." J. Cell Biol. **149**: 153-166.

Katayama, H., H. Zhou, et al. (2001). "Interaction and feedback regulation between STK15/BTAK/Aurora-A kinase and protein phosphatase 1 through mitotic cell division cycle." J. Biol. Chem. **276**: 46219-46224.

Kufer, T. A., H. H. W. Silljé, et al. (2002). "Human TPX2 is required for targeting Aurora-A kinase to the spindle." J. Cell Biol. **158**: 617-623.

Mack, G. J. and D. A. Compton (2001). "Analysis of mitotic microtubuleassociated proteins using mass spectrometry identifies astrin, a spindle-associated protein,." Proc. Natl. Acad. Sci. USA **97**: 14352-14357.

Matsumoto, Y., K. Hayashi, et al. (1999). "Cyclin dependent kinase 2 (CDK2) is required for centrosome duplication in mammalian cells." Curr. Bio. **9**: 429-432.

McNally, F. J., K. Okawa, et al. (1996). "Katanin, the microtubule-severing ATPase, is concentrated at centrosomes." J. Cell Sci. **109**: 561-567.

Mendez, R., L. E. Hake, et al. (2000). "Phosphorylation of CPE binding factor by Eg2 regulates translation of c-mos mRNA." Nature **404**: 302-307.

Meraldi, P., J. Lukas, et al. (1999). "Centrosome duplication in mammalian somatic cells requires E2F and Cdk2-cyclin A." Nature Cell Bio. **1**: 88-93.

Merdes A, R. K., Vechio JD, Cleveland DW. (1996). "A complex of NuMA and cytoplasmic dynein is essential for mitotic spindle assembly." Cell **87**: 447-458.

Miyoshi, Y., K. Iwao, et al. (2001). "Association of centrosomal kinase STK15/BTAK mRNA expression with chromosomal instability in human breast cancers." Int. J. Cancer **92**: 370-373.

Mountain V, S. C., Howard L, Ando A, Schatten G, Compton DA. (1999). "The kinesin-related protein, HSET, opposes the activity of Eg5 and cross-links microtubules in the mammalian mitotic spindle." J. Cell Biol. **147**(351-366).

Rieder, C. L., S. Faruki , et al. (2001). "The centrosome in vertebrates: more than a microtubule-organizing center." Trends Cell Biol. **11**: 413-419.

Sen, S., H. Zhou, et al. (2002). "Amplification/overexpression of a mitotic kinase gene in human bladder cancer." J. Natl. Cancer. Ins. **94**: 1320-1329.

Sharp, D. J., G. C. Rogers, et al. (2000). "Microtubule motors in mitosis." Nature **407**: 41-47.

Specht, K. M. and K. Shokat, M. (2002). "The emerging power of chemical genetics." Curr. Opin. Cell Biol. **14**: 155-159.

Stearns, T. (2001). "Centrosome duplication. a centriolar pas de deux." Cell **105**: 417-420.

Tanaka, T., M. Kimura, et al. (1999). "Centrosomal kinase AIK1 is overexpressed in invasive ductal carcinoma of the breast." Cancer Res. **59**: 2041-2044.

Tsai, T. Y., C. Wiese, et al. (2003). "A Ran signalling pathway mediated by the mitotic kinase Aurora A in spindle assembly." Nature Cell Biol. **5**: 242-248.

Verde, F., J. M. Berrez, et al. (1991). "Taxol-induced microtubule asters in mitotic extracts of Xenopus eggs: requirement for phosphorylated factors and cytoplasmic dynein." J. Cell Biol. **112**: 1177-1187.

Walter, A., O,, W. Seghezzi, et al. (2000). "The mitotic serine/threonine kinase Aurora2/AIK is regulated by phosphorylation and degradation." Oncogene **19**: 4906-4916.

Wilson, P. G., M. T. Fuller, et al. (1997). "Monastral bipolar spindles: implications for dynamic centrosome organization." J. Cell Biol. **110**: 451-464.

Wittmann, T., M. Wilm, et al. (2000). "TPX2, A novel Xenopus MAP involved in spindle pole organization." J. Cell Biol. **149**: 1405-1418.

Zheng, Y., M. K. Jung, et al. (1991). "g-Tubulin is present in *Drosophila melanogaster* and *Homo sapiens* and is associated with the centrosome." Cell **65**: 817-823.

Zhou, H., J. Kuang, et al. (1998). "Tumor amplified kinase *STK15/BTAK* induces centrosome amplification, aneuploidy and transformation." Nature Genetics **20**: 189-93.

Appendices:

Jian Du, Gregory J. Hannon (2002). The centrosomal kinase Aurora-A/STK15 interacts with a putative tumor suppressor NM23-H1. *Nuclei Acid Research*, 30: 5465-5475

Jian Du, Gregory J. Hannon (2004). Suppression of p160ROCK bypass cell cycle arrest following Aurora-A/STK15 depletion. *Proceeding of National Academy of Sciences*, 101:8975-8980

Nucleic Acids Research, 2002, Vol. 30, No. 24 5465–5475

The centrosomal kinase Aurora-A/STK15 interacts with a putative tumor suppressor NM23-H1

Jian Du and Gregory J. Hannon*

Cold Spring Harbor Laboratory, Watson School of Biological Sciences, 1 Bungtown Road, Cold Spring Harbor, NY 11724, USA

Received as resubmission August 19, 2002; Revised and Accepted October 15, 2002

ABSTRACT

Alterations in the activity of the centrosomal kinase, Aurora-A/STK15, have been implicated in centrosome amplification, genome instability and cellular transformation. How STK15 participates in all of these processes remains largely mysterious. The activity of STK15 is regulated by phosphorylation and ubiquitin-mediated degradation, and physically interacts with protein phosphatase 1 (PP1) and CDC20. However, the precise roles of these modifications and interactions have yet to be fully appreciated. Here we show that STK15 associates with a putative tumor and metastasis suppressor, NM23-H1. STK15 and NM23 were initially found to interact in yeast in a two-hybrid assay. Association of these proteins in human cells was confirmed by co-immunoprecipitation from cell lysates and biochemical fractionation indicating that STK15 and NM23-H1 are present in a stable, physical complex. Notably, SKT15 and NM23 both localize to centrosomes throughout the cell cycle irrespective of the integrity of the microtubule network in normal human fibroblasts.

INTRODUCTION

Correct partitioning of the genome during mitosis depends upon the tightly regulated function of the mitotic spindle, which is composed of centrosomes, microtubules, molecular motors, chromosomes and kinetochores. The centrosome is the major microtubule-organizing center in mammalian cells and the counterpart to the spindle pole body of the yeast *Saccharomyces cerevisiae*. The centrosome in mammalian cells is composed of two perpendicularly positioned centrioles and the surrounding amorphous pericentriolar material. γ-Tubulin and pericentrins are constitutive components of the centrosome, while other proteins, such as p53, pRB, BRCA1, BRCA2 and CDK2, accumulate at centrosomes in a cell cycle-dependent manner (1–4).

The centrosome normally duplicates once per cell cycle. This process is initiated during G_1 after cells pass the restriction point and is completed during G_2. Centrosomes separate at G_2/M, migrating to opposite poles of the cell to establish the microtubule network that is required to separate condensed chromosomes during M phase. Centrosomes play a vital role in establishing spindle bipolarity, in assembling spindle microtubules and in determining the plane of cytokinesis (for reviews see 5–10). More recently, accumulating evidence suggests a more direct role than had previously been appreciated for the centrosome in cytokinesis and cell cycle progression during the following G_1 and S phases (11–13).

Centrosome abnormalities, including morphological alterations, supernumerary centrosomes and acentriolar centrosomes, have been demonstrated in most human cancer cells, including those derived from breast, prostate, lung, colon and brain (for reviews see 14,15; see also 2,16–18). Several oncogenes, tumor suppressor genes, cell division cycle and mitotic checkpoint genes are required for or involved in centrosome duplication, such as Ras, BRCA1 and BRCA2, CDK2, cyclin A and ATR (3,19–23). Like other cellular processes, protein kinases play critical roles in the centrosome duplication process. Among the centrosome-associated kinases, Aurora-A/AIK1/BTAK/STK15 kinase has been identified as a candidate oncogene with connections to the centrosome cycle (24–27). Aurora-A/STK15 is overexpressed at both the mRNA and protein levels in a number of cancer cell lines, including breast, ovarian and prostate (25,27), and also in breast cancer tissues (28–30). Its kinase activity peaks at the G_2/M phase of the cell cycle (25). A mutant, kinase-inactive STK15 (Stk15 K162M) abolishes the oncogenic activity of STK15 in Rat1 fibroblasts, while a mutation conferring constitutive activation (Stk15 T288D) increases the kinase activity and enhances transforming potential (25). These results strongly suggest that the kinase activity of STK15 is essential for STK15 function *in vivo*. STK15 is regulated by phosphorylation and ubiquitin-mediated degradation and interacts with CDC20 and protein phosphatase 1 (PP1) (31–35).

As a putative tumor suppressor, the *nm23* gene was discovered on the basis of its reduced expression in highly metastatic cell lines (36). Several studies have shown that NM23 overexpression can reduce the metastatic potential of melanoma and breast carcinoma cells *in vivo* (37–39). Furthermore, nm23 expression, at both the protein and mRNA levels, inversely correlates with high metastatic potential in numerous human cancers, including breast, gastric, cervical and ovarian carcinoma and melanoma (for a review see 40).

*To whom correspondence should be addressed. Tel: +1 516 367 8889; Fax: +1 516 367 8874; Email: hannon@cshl.org

The *nm23* genes encode a protein family with eight subfamilies in human (41). The well characterized biochemical activities of these proteins include NDP kinase (42), protein histidine kinase, histidine-dependent protein phosphotransferase (43–45) and serine autophosphorylation (46,47). Data suggest that it is the level of autophosphorylation that correlates with tumor suppression by NM23 in melanoma cells (46). NM23 associates with the cytoskeleton through an interaction with β-tubulin (48). Awd, the fly homolog of NM23, co-localizes with microtubules in *Drosophila* cells (49) and more recent data have indicated that NM23 may also be a component of the centrosome (50).

Despite the strong evidence that STK15/Aurora-A/BTAK regulates centrosome duplication, cellular transformation and aneuploidy, little evidence directly connects this kinase with known oncogenes or tumor suppressors. Here we provide the data that STK15 interacts with the tumor suppressor NM23, both in yeast and in normal human fibroblasts. NM23 and STK15 co-fractionate in a high molecular weight complex and co-localize at centrosomes throughout the cell cycle.

MATERIALS AND METHODS

Plasmids and primers

Full-length STK15 was obtained by PCR from plasmid pcDNA3-STK15/BTAK (a kind gift from Dr S. Sen; 27) using the primers STK15-CHIS5 (CGGGATCCCGGGGATGGACCGATCTAAAGAAACTGC) and STK15-3XhoI (CCGCTCGAGCTAAGACTGTTTGCTAGCTGATTC). STK15-GBT8 was constructed by cloning into the *Bam*HI and *Xho*I sites of pGBT8. A HeLa cDNA two-hybrid library was used in the two-hybrid screen (51). Full-length nm23-H1 cDNA was obtained by PCR of EST clones ordered from Genome Systems Inc. (EST clones 590228 and 3454119) using the primers NM23GAD-5EcoRI (CGGAATTCCATGGCCAACTGTGA-GCG) and NM23-3XhoI (CCGCTCGAGTCATTCATAGATCCAG). pGADGH-NM23-H1 was constructed by cloning the the PCR product into the *Eco*RI and *Xho*I sites of pGADGH (51).

Cell culture

Human IMR90 cells were purchased from ATCC (CCL-186). These were immortalized by infection with a hTERT retrovirus at passage 25 (52). The cells were cultured at 37°C in a 5% CO_2 incubator in Dulbecco's modified medium (DMEM) supplemented with 10% (v/v) heat-inactivated fetal bovine serum (FBS), 10% (v/v) non-essential amino acids (NEAA) and penicillin/streptomycin (100 IU/ml and 100 µg/ml, respectively). Nocodazole treatment was done by addition of 10 µg/ml nocodazole to the culture medium followed by incubation for 10 min at 37°C.

Two-hybrid screening

To identify proteins interacting with STK15, we screened a plasmid library of fusions between the GAL4 activation domain (GAD, residues 768–881) and HeLa cell cDNA fragments. The Gal4 DNA-binding domain (GBD) is fused with STK15 in the pSTK15-GBT8 construct. The screen was done in a *S.cerevisiae* reporter strain (pJ64-4a, W303*MAT*a *trp9-901, 112 ura3-52 his3-200 gal4 gal80 GAL2-ADE2 LYS2::GAL1-HIS3 met2::GAL7-LacZ*, a kind gift from R. Rothstein). A total of 1.2×10^6 transformants were assayed on synthetic drop-out medium (without leucine, histidine and tryptophan, SC –HLW) plates. A total of 104 colonies turned blue on X-gal plates, and the plasmids were recovered from 54 colonies. Retransformation of the plasmids into the test strain confirmed that 20 plasmids retained the ability to activate the β-galactosidase reporter. Sequencing analysis revealed four plasmids contained coding sequences from *nm23-H1* genes. The four plasmids were derived from two independent cDNAs comprising nucleotides 25–330 and 4–159 of the *nm23-H1* coding region.

Antibodies

A polyclonal antiserum against STK15 (anti-STK15) was raised in rabbits by presenting a KLH-conjugated nine amino acid peptide (synthesized by Research Genetics, Huntsville, AL) from the C-terminus of STK15 (NKESASKQS). The serum was affinity purified using a resin prepared from the synthesized peptide (53). The antibody recognizes a 46 kDa band in whole cell lysates. For some studies, the affinity-purified antibody was labeled with Alexa Fluor 647 dye (Molecular Probes, Eugene, OR), for example for examination of cells triple labeled by anti-β-tubulin-FITC, anti-NM23-H1-TRITC and anti-STK15-AF647 antibodies. Affinity-purified anti-NM23 antibodies were obtained from Santa Cruz Biotechnology (Santa Cruz, CA) (rabbit polyclonal sc-343 and sc-343-TRITC for immunofluorescence and mouse monoclonal sc-465 for immunoprecipitation). Mouse monoclonal anti-centrin2 antibody was a kind gift from Dr J. L. Salisbury (Mayo Clinic, Rochester, MN). Monoclonal anti-γ-tubulin (T-3195) and FITC-conjugated mouse monoclonal anti-β-tubulin were obtained from Sigma (St Louis, MO). Secondary antibodies were obtained from Pierce (Rockford, IL), Jackson Immunoresearch Laboratory Inc. (West Grove, PA) and Molecular Probes Inc. (Eugene, OR).

Immunoblotting, immunoprecipitation and fluorescence microscopy

IMR90 cells were lysed in IP buffer [125 mM NaCl, 1 mM $Mg(OAc)_2$, 1 mM $CaCl_2$, 5 mM EGTA, 20 mM HEPES (pH 7.6), 1% (v/v) NP-40, with freshly dissolved 2 mM DTT, 0.2 mM phenylmethylsulfonyl fluoride and protease inhibitors (Roche, Mannheim, Germany)] on ice for 10–15 min. Protein concentrations were determined by Bradford assay (Bio-Rad). A total of 10–50 µg protein was analyzed by 10 or 12% (v/v) SDS–PAGE (54).

Immunoprecipitation was performed as described (55) with the following modifications. IMR90 cells were lysed in IP buffer at 4°C for 10 min. The cell lysate was cleared by centrifugation at 10 000 *g* for 10 min at 4°C. The supernatant was pre-cleared by incubation for 30 min with agarose–protein A or agarose–protein G beads (Pierce). The supernatant was further incubated with 5 µg antibodies for 3–4 h at 4°C with agitation, after which agarose–protein A or A/G mixture (pre-blocked by incubation with 5% BSA) was added for 1 h at 4°C. The beads were then washed three times with IP buffer. For release of STK15 and associated proteins, beads were incubated with 1 mg/ml synthetic antigen in phosphate-buffered saline (PBS) for 1 h at 4°C with agitation.

For indirect immunofluorescence, cells were grown on acid-washed 13 mm square glass coverslips (Fisher Scientific, Pittsburgh, PA). Cells were first fixed with 0.5% (w/v) formaldehyde in PBS (pH 7.2) for 15 min at room temperature and then washed four times with PBS. Fixed cells were permeabilized by 0.1% (v/v) Triton X-100 in PBS with 1% (v/v) normal goat serum (NGS) and then washed with PBS with 1% (v/v) NGS (Gibco-BRL). The primary antibodies used were anti-STK15 1:100, anti-NM23 1:200, anti-centrin2 1:200 and anti-β-tubulin-FITC 1:25, at room temperature for 1 h. Secondary antibodies were diluted in the blocking buffer at 1:100 or 1:200 and incubated for 1 h at room temperature in the dark. The first wash after secondary antibody included 1 μg/ml Hoechst 33342 (Sigma) for 15 min at room temperature. For triple labeling, the primary antibodies used were as follows: anti-β-tubulin-FITC 1:25, anti-NM23-TRITC 1:50 and anti-STK15-AF647 1:50. Coverslips were mounted on glass slides with mounting medium. Microscopy was carried out on Nikon or Zeiss microscopes with 63× or 100× oil immersion lens. The images were captured with Openlab (Lexington, MA) software and saved as TIFF files.

Biochemical fractionation of STK15 and NM23

For fractionation of STK15 and NM23, IMR90 cells were lysed as above and the lysates were cleared by centrifugation at 10 000 *g* for 10 min at 4°C. The supernatants were cleared by passage through a 0.2 μm filter and fractionated through three chromatographic steps, Mono S, Mono Q and Superose 6 HR10/30 (Amersham-Pharmacia Biotech, Piscataway, NJ), in an AKAT FPLC system. The cell lysates were loaded first on Mono S and eluted with a linear gradient of from 100 to 1000 mM potassium chloride in MonoS buffer [20 mM HEPES (pH 7.6), 10% (v/v) glycerol, 1 mM DTT, 1 mM EDTA, 0.01% (v/v) NP40]. Fractions were collected (0.5 ml) and those containing the peak of STK15 1.5 ml (from 280 to 370 mM) were collected and dialyzed against MonoQ buffer [20 mM HEPES (pH 8.0), 10% (v/v) glycerol, 1 mM DTT, 1 mM EDTA, 0.01% (v/v) NP40, containing 100 mM NaCl]. The dialyzed eluate was then loaded onto Mono Q and was eluted with a linear gradient from 0 to 1000 mM potassium chloride in MonoQ buffer. The peak fractions for STK15 (from 350 to 450 mM) were collected and pooled before 0.5 ml was loaded onto Superose 6. The column was run at 0.4 ml/min with Super6 buffer [20 mM HEPES (pH 7.6), 10% (v/v) glycerol, 1 mM DTT, 1 mM EDTA, 0.01% NP40 and 300 mM NaCl]. Fractions of 1 ml were collected and proteins were precipitated with TCA. The pellets were then re-dissolved in 0.1 N NaOH and loaded onto SDS–PAGE gels for immunoblot analysis.

RESULTS AND DISCUSSION

NM23 and STK15 interact

To search for proteins that interact with STK15 we conducted a yeast two-hybrid screen using the full-length STK15 coding sequence as a bait (see Materials and Methods). Among the positives, we found four plasmids containing the human *nm23-H1* coding sequence. Two different fusions were represented, which cover a common N-terminal region of NM23-H1 (three represented fusions of Gal4 to amino acids 9–110, and another represented amino acids 2–53). This suggests that the region of NM23-H1 between amino acids 2 and 53 binds directly to STK15. We inserted the full-length *nm23-H1* coding sequence into pGADGH (pGADGH-NM23-H1) and confirmed that this fusion protein also interacts specifically with STK15 (Fig. 1). Only in combination with STK15 did colonies carrying NM23-H1 show significant β-galactosidase expression. Neither NM23-H1 alone nor NM23 combined with other Gal4 fusion proteins (e.g. ras) induced β-galactosidase expression. However, at least in yeast, the degree of X-gal staining indicated that the interaction between STK15 and Nm-23H1 was relatively weak, as compared to the positive control (pGBT8-Ras and pGADGH-Raf in this case). It was therefore essential to

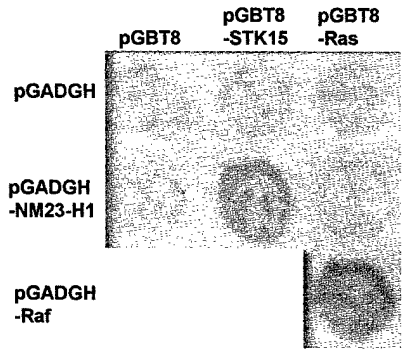

Figure 1. STK15 and NM23 interact specifically in the two-hybrid assay. Transformants of *S.cerevisiae* strain pJ64-4a were grown and re-patched on synthetic complete plates lacking Leu and Trp to select for both pGBT and pGADGH plasmid derivatives. The patches were transferred to Whatman No. 1 filter paper for β-galactosidase assays and the color was developed at 37°C for 1 h. A combination of pGBT8-Ras and pGADGH-Raf served as the positive control.

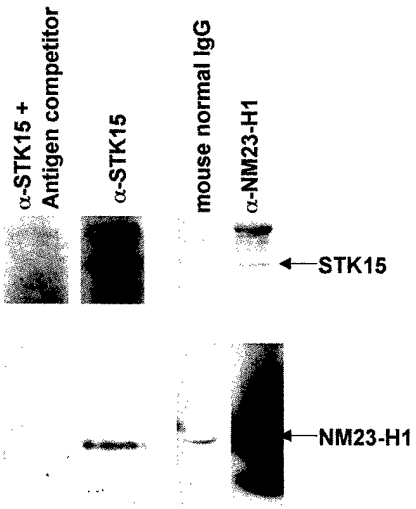

Figure 2. STK15 and NM23 co-immunoprecipitate. Protein lysates from immortalized IMR90 cells were cleared by centrifugation and immunoprecipitated with anti-STK15 plus STK15 polypeptide antigen competitor (lane 1), anti-STK15 alone (lane 2), normal mouse IgG (lane 3) and anti-NM23-H1 (lane 4). The immunoprecipited proteins were fractionated by SDS–PAGE and transferred to nitrocellulose membrane for western blotting. STK15 and NM23-H1 are indicated by arrows.

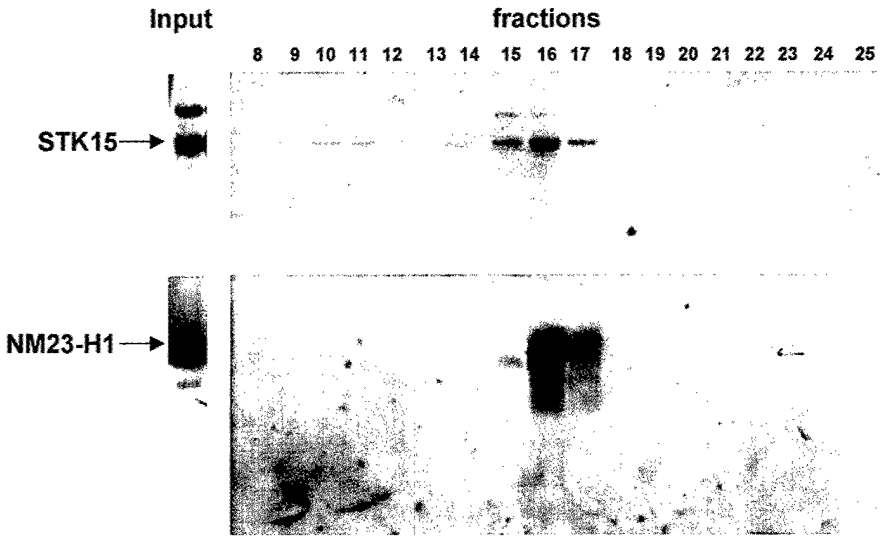

Figure 3. STK15 and NM23-H1 co-fractionate. Protein lysates from immortalized IMR90 cells were fractionated on Mono S, Mono Q and Superose 6 columns. Fractions 8–25 of 1 ml volume were collected after the final Superose 6 gel filtration column and constituent proteins were separated by SDS–PAGE for western blotting. STK15 and NM23-H1 are indicated by arrows.

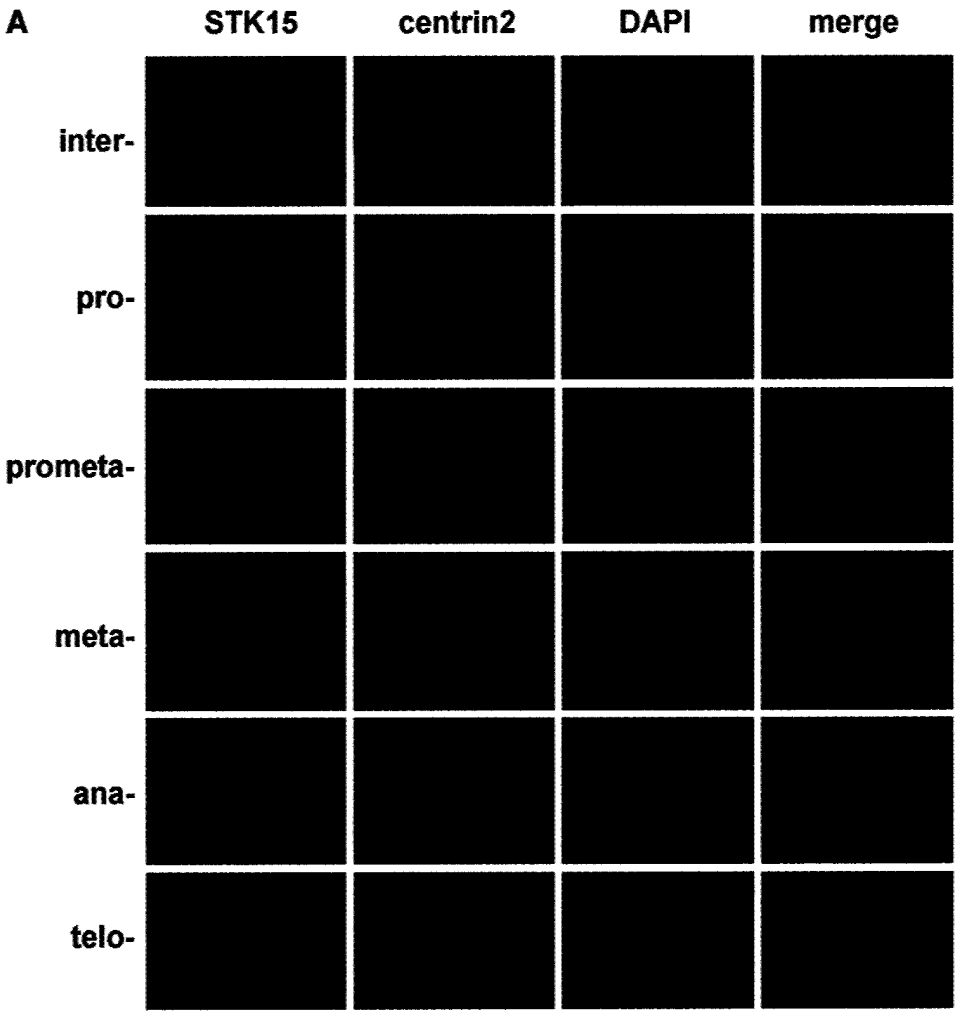

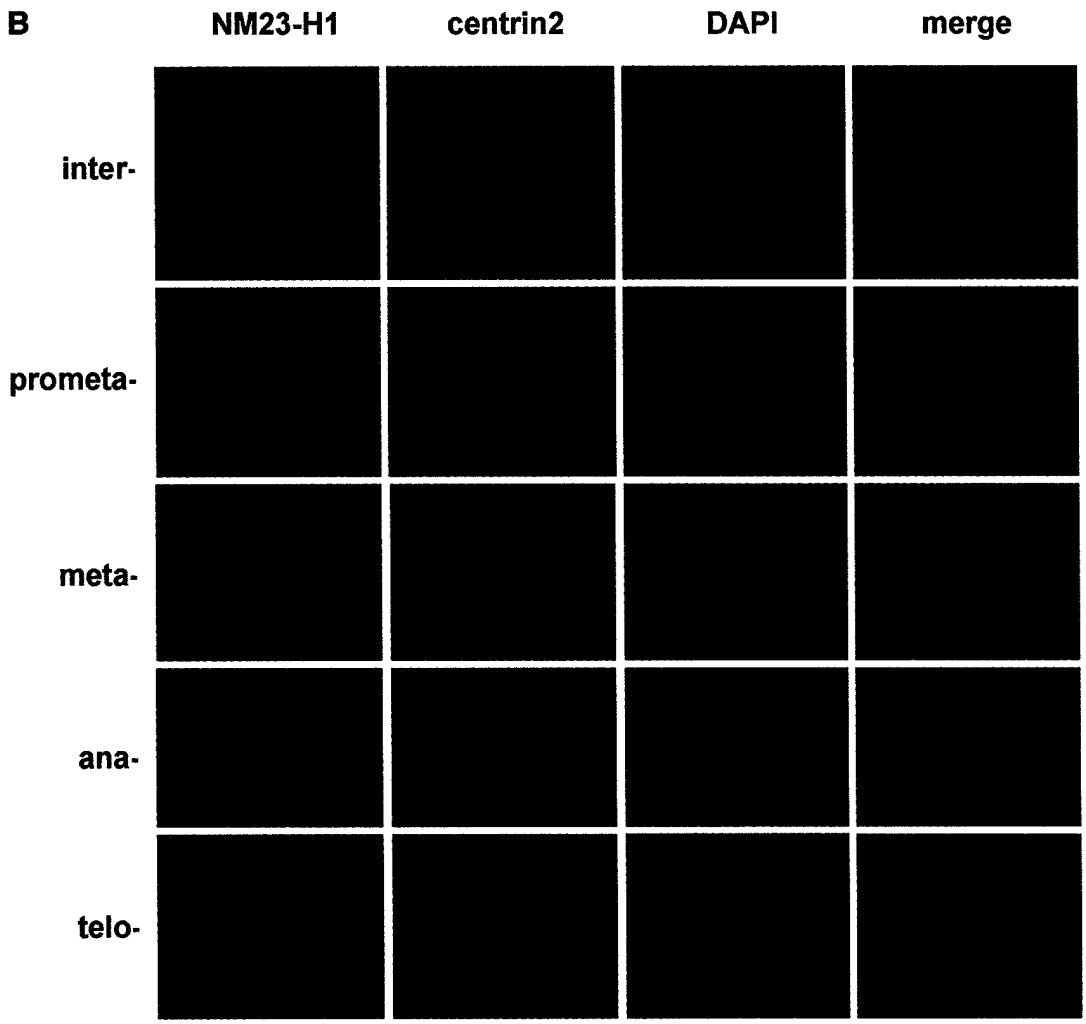

investigate whether these proteins physically interacted in mammalian cells.

To test whether STK15 and NM23 also interact *in vivo* in human cells, proteins were immunoprecipitated from IMR90 cell lysates using anti-STK15 and anti-NM23 antibodies (see Materials and Methods). The presence of NM23 and STK15 in the precipitate was examined by western blotting (Fig. 2). Anti-STK15 specifically co-immunoprecipitates STK15 and NM23. Pre-incubation of the STK15 antibody with its cognate synthetic antigen coordinately abolished immunoprecipitation of both STK15 and NM23 (Fig. 2, lanes 1 and 2). The NM23 antiserum also immunoprecipitated NM23 and STK15, while normal mouse IgG did not bring down significant amounts of either NM23 or STK15 (Fig. 2, lanes 3 and 4). We did detect some non-specific binding of NM23 to protein A/G beads; however, this is not unexpected considering that NM23 is a relatively abundant protein (lane 3). The foregoing results indicate that STK15 and NM23 associate with each other in human cells. Comparing the total amount of NM23 present in the cell and the amount precipitated by anti-NM23-H1 antibody (Fig. 2, lane 4, and western data not shown) to the amount of NM23 immunoprecipitated by the STK15 antibody (Fig. 2, lane 2; both lanes 2 and 4 were from the same amount of cell lysate) suggests that a relatively small percentage of NM23-H1 exists in a stable, physical complex with STK15. In western blots of the anti-STK15 immunoprecipitations, we also detected another protein of ~54 kDa, in addition to the 46 kDa protein that is predicted to be an STK15 protein derived from an alternatively spliced mRNA. We have not definitively determined the identity of the 54 kDa protein; however, the human genome sequencing project has predicted an alternatively spliced STK15 transcript that is predicted to generate a protein of this size (accession no. XP_009546). In contrast, we have confirmed that the ~46 kDa band is STK15 by MALDI-TOF mass spectrometry.

To verify the interaction between STK15 and NM23-H1, protein extracts from IMR90 cells were fractionated by FPLC. Throughout the purification, we followed STK15 by western blotting. Western analysis of the purification through Mono S, Mono Q and Superose 6 columns revealed that STK15 is present in two distinct forms, a high molecular weight protein complex (Fig. 3, fractions 10 and 11, ~2 MDa) and a relatively low molecular weight complex (fractions 15–17, ~350 KDa). NM23-H1 also shows a peak around fractions 15–17, which

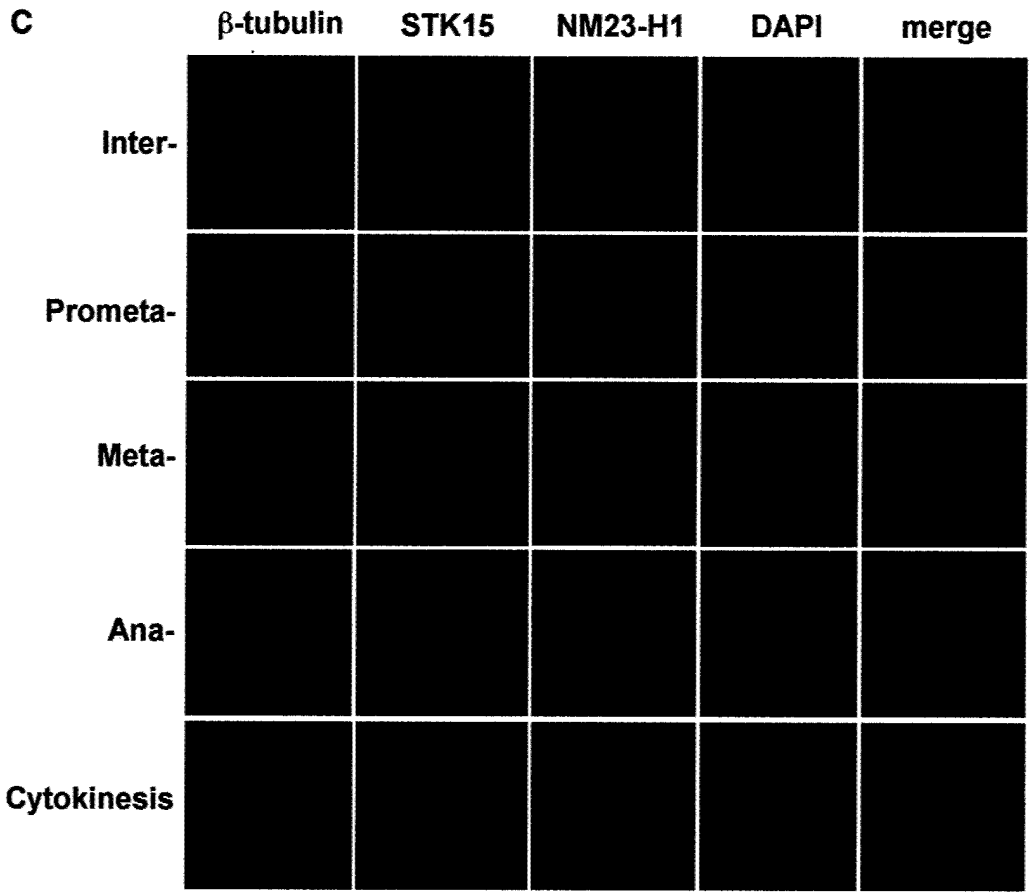

Figure 4. (Previous two pages and above) STK15 and NM23-H1 localize to centrosomes throughout the cell cycle. IMR90 cells were plated on glass coverslips and cultured in growth medium for 24 h before fixation with paraformaldehyde. The centrosome was visualized with anti-centrin2 and Texas red-labeled secondary antibodies. (**A**) STK15 and (**B**) NM23-H1 were visualized with anti-STK15 and anti-NM23-H1, respectively, and FITC-labeled secondary antibodies. DNA was labeled by Hoechst 33342 or DAPI staining. The composite images are STK15 or NM23 merged with centrin2 and DAPI. The green NM23 or STK15 merged with red centrin2 produces yellow spots in the composite image, indicating that NM23 and STK15 localize to the centrosomes. (**C**) Cells were labeled with anti-β-tubulin-FITC, anti-NM23-TRITC and anti-STK15-AF647 (Cy5) simultaneously and visualized on the microscope with FITC, TRITC, Cy5 and DAPI filters, respectively. Cell cycle stages are indicated on the left.

exactly co-migrates with STK15 in the ~350 kDa complex (Fig. 3). This result supports the notion that STK15 and NM23 coexist in a protein complex *in vivo*.

STK15 and NM23 co-localize at centrosomes

It has been shown that STK15 localizes to centrosomes in mitotic cells (25) (Fig. 4A). By fixing IMR90 cells in 0.5% (w/v) formaldehyde, we can also detect STK15 at centrosomes during interphase in immortalized human IMR90 cells. Centrosomes were visualized by simultaneous staining with an anti-centrin2 antiserum, which locates the two centrioles in the centrosome (Fig. 4). The amount of STK15 at centrosomes increases as cells move from interphase to prophase, and SKT15 also becomes apparent on the mitotic spindle. These results suggest that STK15 is a centrosome component throughout the cell cycle (Fig. 4A), but becomes enriched at centrosomes during mitosis. NM23-H1 also localizes to centrosomes in interphase cells (Fig. 4B) (50). At the beginning of prophase NM23-H1 accumulates at the centrosome, as judged from the increased intensity of staining (Fig. 4B, prometaphase) (50). The association of NM23 with centrosomes persists through the mitotic phase and NM23-H1 also distributes somewhat to the microtubule spindles adjacent to the centrosome from metaphase to telophase (Fig. 4B) (50). From late telophase to cytokinesis, NM23-H1 also accumulates at the newly forming midbody microtubules (Figs 4C and 5C in late telophase and cytokinesis cells). Interestingly, an identical distribution pattern at the midbody microtubules is also observed for STK15 (Figs 4C and 5B in late telophase and cytokinesis cells). The accumulation of NM23-H1 on centrosomes coincides with the enrichment of STK15 at the centrosome and with increased STK15 kinase activity at the beginning of mitosis (25).

In order to test whether STK15 and NM23 co-localize, we simultaneously labeled IMR90 cells with β-tubulin-FITC, NM23-TRITC and STK15-AF647 (Cy5) and visualized the localization of each protein (Fig. 4C). β-Tubulin immunofluorescence reveals interphase microtubule filaments and centrosomes. In mitotic phase, β-tubulin localizes both to the mitotic spindles and to the centrosomes (Fig. 4C). NM23 and

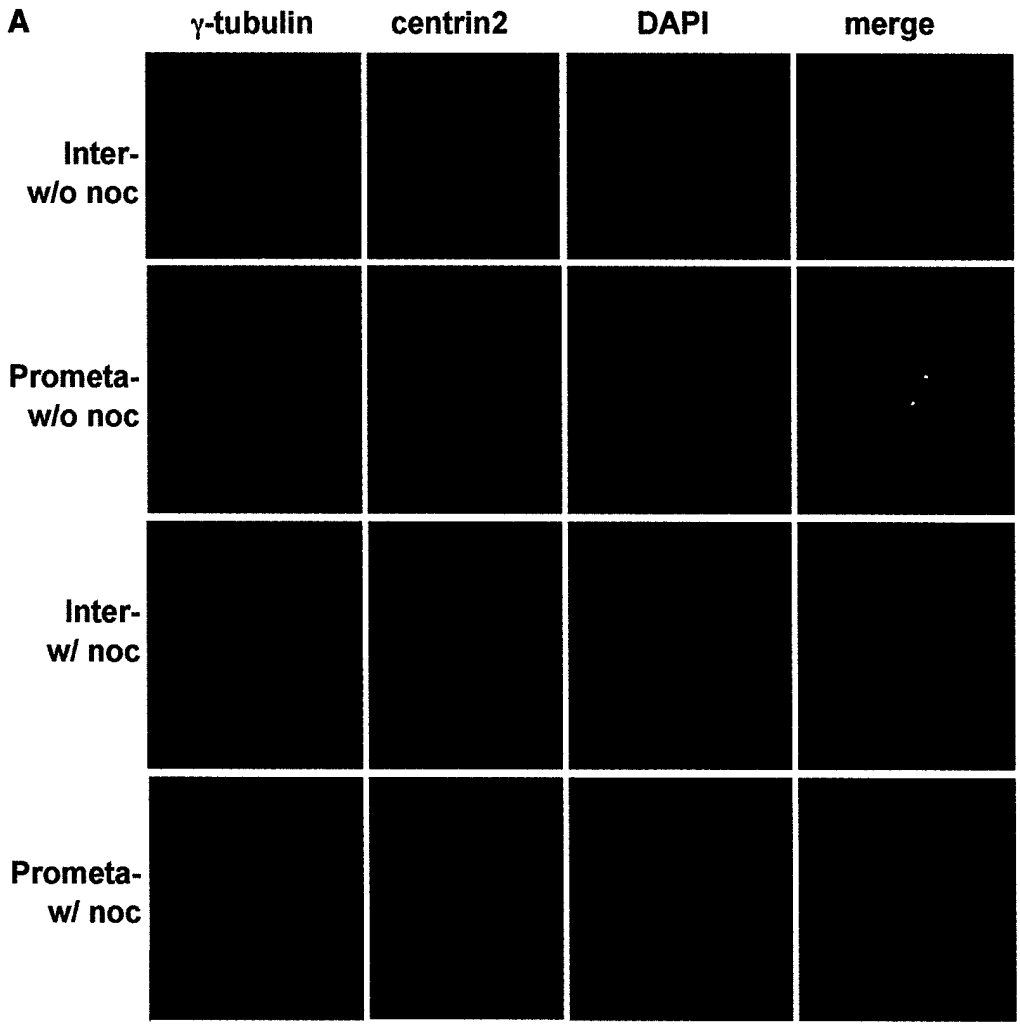

STK15 fluorescence is present together at the centrosome at all cell cycle phases (Fig. 4C, the right side merged lane). These results confirm that STK15 and at least some fraction of NM23 co-localize to centrosomes throughout the cell cycle.

STK15 and NM23 centrosomal localization is microtubule-independent

There is some evidence indicating that NM23-H1 is β-tubulin associated and localized through γ-tubulin to centrosomes (48,50). In order to clarify that STK15 and NM23 do not associate indirectly at centrosomes through their separate interactions with microtubules, we treated IMR90 cells with nocodazole (see Materials and Methods), which rapidly dissipates the microtubule network in cells (Fig. 5B and C, β-tubulin column).

There are several centrosome-associated proteins that localize to this structure in a spindle-dependent fashion. Of these, perhaps the most well studied is γ-tubulin (56). Upon nocodazole treatment of mammalian cells, centrosomal γ-tubulin is reduced by ~2-fold in interphase cells and by at least 4-fold in mitotic cells (56). Using β- and γ-tubulin antisera, we confirmed that our nocodazole treatment dissipates the microtubule network and dramatically reduces the amount of γ-tubulin associated with the centrosome (Fig. 5A–C). In such cells, STK15 and NM23-H1 still localize to the centrosome with the same pattern and intensity of staining seen in untreated cells (Fig. 5B and C). The result suggests that the interaction between STK15 and NM23 and their centrosome localization are microtubule-independent.

A previous study (57) showed that the centrosomal localization of a *Xenopus laevis* homolog of STK15, Aurora-A, is microtubule-dependent. This result was obtained using a construct consisting of the only N-terminal domain of Aurora-A (57). However, microtubule-independent localization of Aurora-A to the centrosome was observed using a full-length Aurora-A construct (57). Here, we also observed that the localization of full-length STK15 to the centrosome is not dependent on microtubules (Fig. 5B).

A previous study showed that STK15 associates with centrosomes only at onset of mitosis (25). However, our immunofluorescence studies indicate that STK15 associates with centrosomes throughout the cell cycle. This discrepancy

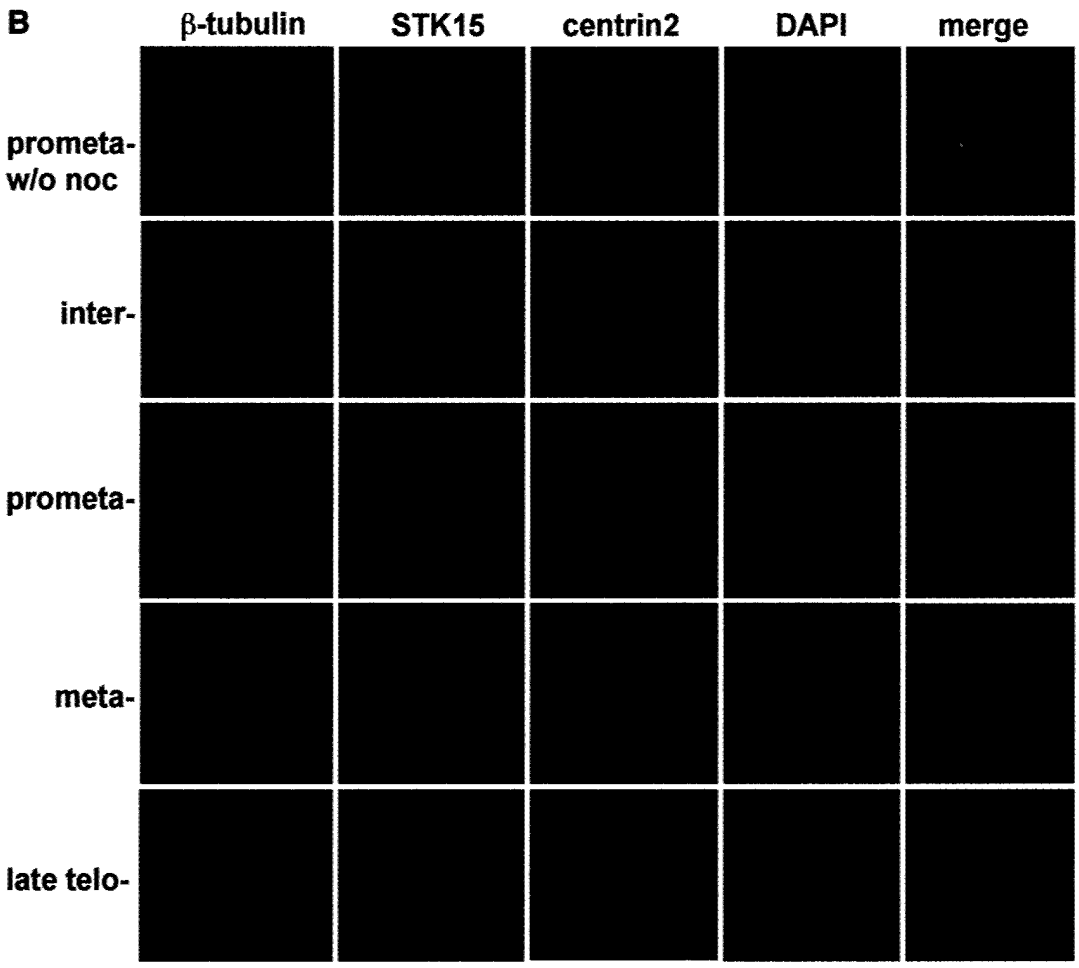

could arise because of the different cell types used in these studies. Here we examined STK15 in normal or immortalized human fibroblasts cells while previous studies have used human cancer cells and rodent fibroblast cells. Furthermore, different antisera and fixation conditions were used in this and in previous studies. We do, however, observe an increase in the abundance of STK15 at centrosomes in mitotic cells.

STK15 is a centrosome-associated kinase, overexpression of which in rodent or human cancer cells causes improper centrosome duplication, aneuploidy and cellular transformation (25,27). The abundance of STK15 is controlled by the ubiquitin pathway (32,33) and has been linked to CDC20, an APC activator (31). STK15 kinase activity is also controlled by PP1, a protein phosphatase (34). Here we provide evidence that STK15 is associated with a putative tumor and metastasis suppressor protein, NM23-H1. These proteins physically interact and co-localize to centrosomes throughout the cell cycle in human IMR90 cells. NM23-H1 plays important roles in cell proliferation, differentiation, tumorigenesis and metastasis.

The interaction between NM23 and STK15 might potentially modulate either of their activities through a number of mechanisms, ranging from allosteric regulation to induced localization to enzymatic modification. We tested the latter possibility using STK15 and NM23-H1, purified from *Escherichia coli*. Purified STK15 was enzymatically active, as judged by its ability to phosporylate a model substrate, MBP. NM23 also displayed activity as judged by autophosphorylation and NDP kinase activities (data not shown; 46,58). Neither of the purified proteins was capable of chemically modifying the other nor did mixing these proteins affect their activities towards model substrates *in vitro*. Therefore, the exact nature of the functional relationship between NM23 and SKT15 remains unknown.

ACKNOWLEDGEMENTS

We would like to thank J. L. Salisbury (Mayo Clinic, Rochester, MN) for the kind gift of the anti-centrin2 antiserum, S. Sen (University of Texas M.D. Anderson Cancer Center, Houston, TX) for the STK15 plasmid, R. Rothstein (Columbia University) for the yeast two-hybrid strain pJ64-4a and Y. Seger (Cold Spring Harbor) for the hTERT retroviral plasmid. The authors would also like to thank D. Conklin, M. Carmell, S. Hammond, A. Caudy and other members in the laboratory for technical support and helpful discussions. We are thankful to Stephen Hearn and Gayle Lark at the core microscopy facility and Jim Duffy in

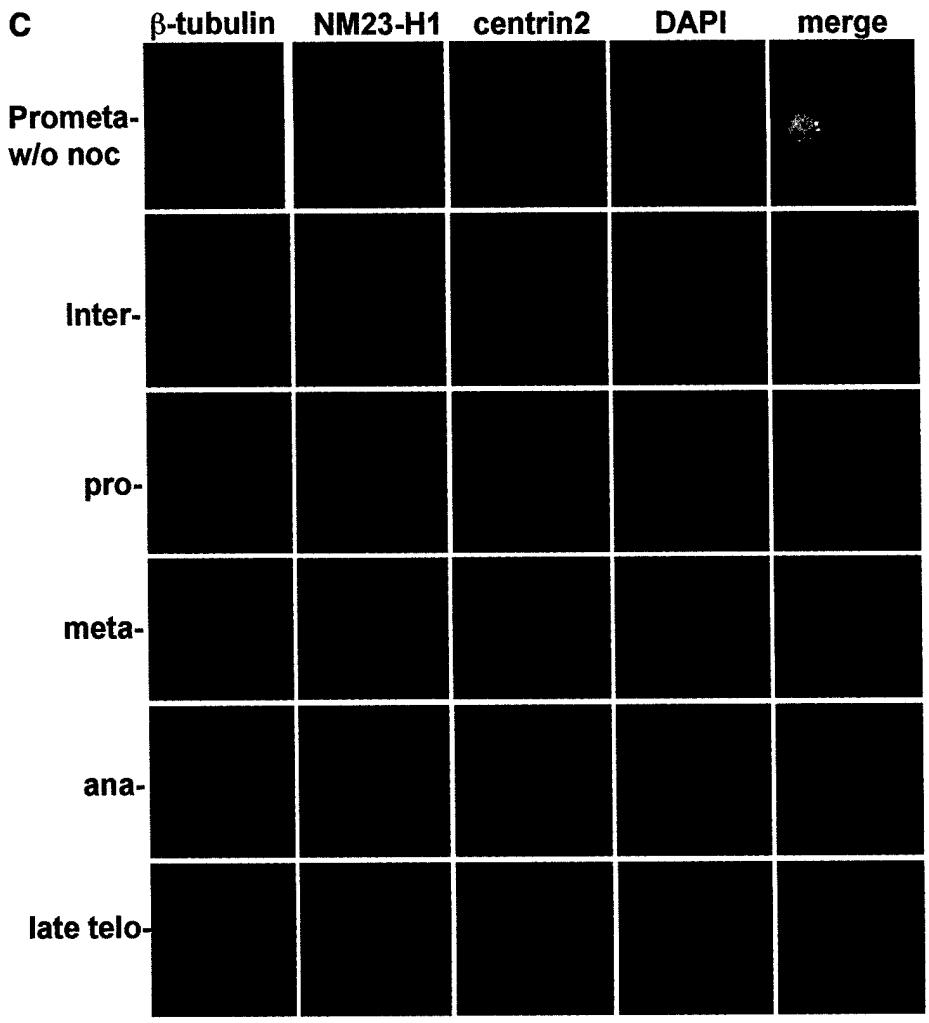

Figure 5. (Previous two pages and above) The centrosome localization of STK15 and NM23-H1 is not microtubule dependent. (**A**) IMR90 cells grown on coverslips were treated with or without nocodazole and fixed for immunofluorescence. The centrosome was visualized by staining with anti-centrin2 and anti-γ-tubulin antibodies. As predicted, the signal representing centrosome-associated γ-tubulin becomes significantly weakened, especially in mitotic cells (prometaphase cells here), upon nocodazole treatment (labeled w/ noc on the left), as compared to that seen in cells without nocodazole (labeled w/o noc on the left). (**B**) STK15 and (**C**) NM23-H1 still localize to centrosome in nocodazole-treated cells throughout the cell cycle. IMR90 cells treated with or without nocodazole (w/o noc) were fixed and triple labeled for β-tubulin (FITC), STK15/NM23-H1 (Cy5), centrin2 (Texas red) and DNA (DAPI). The nocodazole treatment totally dissipates the microtubule spindles so the cells with nocodazole fail to show the characteristic β-tubulin staining pattern (the β-tubulin columns). Cell cycle stages are indicated on the left.

the art department. J.D. is supported by a post-doctoral fellowship (PC001528) from the Department of Defense Prostate Cancer Research Program (PCRP). This work was supported by a grant from the NIH (P01-CA13106) to G.J.H.

REFERENCES

1. Zheng,Y., Jung,M.K. and Oakley,B.R. (1991) γ-Tubulin is present in *Drosophila melanogaster* and *Homo sapiens* and is associated with the centrosome. *Cell*, **65**, 817–823.
2. Carroll,P.E., Okuda,M., Horn,H.F., Biddinger,P., Stambrook,P.J., Gleich,L.L., Li,Y.,Q., Tarapore,P. and Fukasawa,K. (1999) Centrosome hyperamplification in human cancer: chromosome instability induced by p53 mutation and/or Mdm2 overexpression. *Oncogene*, **18**, 1935–1944.
3. Hsu,L.C. and White,R.L. (1998) BRAC1 is associated with the centrosome during mitosis. *Proc. Natl Acad. Sci. USA*, **95**, 12983–12988.
4. Matsumoto,Y., Hayashi,K. and Nishida,E. (1999) Cyclin dependent kinase 2 (CDK2) is required for centrosome duplication in mammalian cells. *Curr. Biol.*, **9**, 429–432.
5. Lange,B.M. (2002) Integration of the centrosome in cell cycle control, stress response and signal transduction pathways. *Curr. Opin. Cell Biol.*, **14**, 35–43.
6. Bornens,M. (2002) Centrosome composition and microtubule anchoring mechanisms. *Curr. Opin. Cell Biol.*, **14**, 25–34.
7. Rieder,C.L., Faruki,S. and Khodjakov,A. (2001) The centrosome in vertebrates: more than a microtubule-organizing center. *Trends Cell Biol.*, **11**, 413–419.
8. Hinchcliffe,E.H. and Sluder,G. (2001) Centrosome duplication: three kinases come up a winner! *Curr. Biol.*, **11**, R698–R701.
9. Doxsey,S. (2001) Re-evaluating centrosome function. *Nature Rev. Mol. Cell Biol.*, **2**, 688–698.
10. Stearns,T. (2001) Centrosome duplication. A centriolar pas de deux. *Cell*, **105**, 417–420.
11. Hinchcliffe,E.H., Miller,F.J., Cham,M., Khodjakov,A. and Sluder,G. (2001) Requirement of a centrosomal activity for cell cycle progression through G1 into S phase. *Science*, **291**, 1547–1550.

12. Khodjakov,A. and Rieder,C.L. (2001) Centrosomes enhance the fidelity of cytokinesis in vertebrates and are required for cell cycle progression. *J. Cell Biol.*, **153**, 237–242.
13. Piel,M., Nordberg,J., Euteneuer,U. and Bornens,M. (2001) Centrosome-dependent exit of cytokinesis in animal cells. *Science*, **291**, 1550–1553.
14. Salisbury,J.L. (2001) The contribution of epigenetic changes to abnormal centrosomes and genomic instability in breast cancer. *J. Mammary Gland Biol. Neoplasia*, **6**, 203–212.
15. Pihan,G.A., Purohit,A., Wallace,J., Knecht,H., Woda,B., Quesenberry,P. and Doxsey,S.J. (1998) Centrosome defects and genetic instability in malignant tumors. *Cancer Res.*, **58**, 3974–3985.
16. Weber,R.G., Bridger,J.M., Benner,A., Weisenberger,D., Ehemann,V., Reifenberger,G. and Lichter,P. (1998) Centrosome amplification as a possible mechanism for numerical chromosome aberrations in cerebral primitive neuroectodermal tumors with TP53 mutations. *Cytogenet. Cell Genet.*, **83**, 266–269.
17. Gradimi,B.M., Sackett,D.L., Difilippantonio,M.J., Schrock,E., Neumann,T., Jauho,A., Auer,G. and Reid,T. (2000) Centrosome amplification and instability occurs exclusively in aneuploidy, but not in diploid colorectal cancer cell lines, and correlates with numerical chromosomal aberrations. *Genes Chromosomes Cancer*, **27**, 183–190.
18. Marx,J. (2001) Do centrosome abnormalities lead to cancer? *Science*, **292**, 426–427.
19. Saavedra,H.I., Fukasawa,K., Conn,C.W. and Stambrook,P.J. (1999) MAPK mediate ras-induced chromosome instability. *J. Biol. Chem.*, **274**, 38083–38090.
20. Tutt,A., Gabriel,A., Bertwistle,D., Connor,F., Paterson,H., Peacock,J., Ross,G. and Ashworth,A. (1999) Absence of BRCA2 causes genome instability by chromosome breakage and loss associated with centrosome amplification. *Curr. Biol.*, **9**, 1107–1110.
21. Fukasawa,K., Choi,T., Kuriyama,R., Rulong,S. and Vande Woude,G.F. (1996) Abnormal centrosome amplification in the absence of p53. *Science*, **271**, 1744–1747.
22. Hollander,M.C., Sheikh,M.S., Bulavin,D.V., Lundgren,K., Augeri-Henmueller,L., Shehee,R., Molanaro,T.A., Kim,K.T., Tolosa,E., Ashwell,J.D. *et al.* (1999). Genomic instability in gadd45a-deficient mice. *Nature Genet.*, **23**, 176–184.
23. Meraldi,P., Lukas,J., Fry,A.M., Bartek,J. and Nigg,E.A. (1999) Centrosome duplication in mammalian somatic cells required E2F and Cdk2-Cyclin A. *Nature Cell Biol.*, **1**, 88–93.
24. Glover,D.M., Leibowitz,M.H., McLean,D.A. and Parry,H. (1995) Mutations in aurora prevent centrosome separation leading to the formation of monopolar spindles. *Cell*, **81**, 95–105.
25. Bischoff,J.R., Anderson,L., Zhu,Y., Mossie,K., Ng,L., Souza,B., Schryver,B., Flanagan,P., Chairvoyant,F., Ginther,C. *et al.* (1998). A homologue of *Drosophila* aurora kinase is oncogenic and amplified in human colorectal cancers. *EMBO J.*, **17**, 3052–3065.
26. Sen,S., Zhou,H. and White,R.A. (1997) A putative serine/threonine kinase encoding gene BTAK on chromosome 20q13 is amplified and over expressed in human breast cancer cell lines. *Oncogene*, **14**, 2195–2200.
27. Zhou,H., Kuang,J., Zhong,L., Kuo,W., Grey,J., Sahin,A., Brinkley,B. and Sen,S. (1998) Tumor amplified kinase *STK15/BTAK* induces centrosome amplification, aneuploidy and transformation. *Nature Genet.*, **20**, 189–193.
28. Tanaka,T., Kimura,M., Matsunaga,K., Fukada,D., Mori,H. and Okano,Y. (1999) Centrosomal kinase AIK1 is overexpressed in invasive ductal carcinoma of the breast. *Cancer Res.*, **59**, 2041–2044.
29. Miyoshi,Y., Iwao,K., Egawa,C. and Noguchi,S. (2001) Association of centrosomal kinase STK15/BTAK mRNA expression with chromosomal instability in human breast cancers. *Int. J. Cancer*, **92**, 370–373.
30. Shin,S.O., Lee,K.H., Kim,J.H., Baek,S.H., Park,J.W., Gabrielson,E.W. and Kwon,T.K. (2000) Alternative splicing in 5′-untranslational region of STK-15 gene, encoding centrosome associated kinase, in breast cancer cell lines. *Exp. Mol. Med.*, **32**, 193–196.
31. Farruggio,D.C., Townsley,F.M. and Ruderman,J.V. (1999) Cdc20 associates with the kinase aurora2/Aik. *Proc. Natl Acad. Sci. USA*, **96**, 7306–7311.
32. Honda,K., Mihara,H., Kato,Y., Yamaguchi,A., Tanaka,H., Yasuda,H., Furukawa,K. and Urano,T. (2000) Degradation of human Aurora2 protein kinase by the anaphase-promoting complex-ubiquitin-proteasome pathway. *Oncogene*, **19**, 2812–2819.
33. Walter,A.O., Seghezzi,W., Korver,W., Sheung,J. and Lees,E. (2000) The mitotic serine/threonine kinase Aurora2/AIK is regulated by phosphorylation and degradation. *Oncogene*, **19**, 4906–4916.
34. Katayama,H., Zhou,H., Li,Q., Tatsuka,M. and Sen,S. (2001) Interaction and feedback regulation between STK15/BTAK/Aurora-A kinase and protein phosphatase 1 through mitotic cell division cycle. *J. Biol. Chem.*, **276**, 46219–46224.
35. Hannak,E., Kirkham,M., Hyman,A.A. and Oegema,K. (2001) Aurora-1 kinase is required for centrosome maturation in *Caenorhabditis elegans*. *J. Cell Biol.*, **155**, 1109–1115.
36. Steeg,P.S., Bevilacqua,G., Kopper,L., Thorgeirsson,U.P., Talmadge,J.E., Liotta,L.A. and Sobel,M.E. (1988) Evidence for a novel gene associated with low tumor metastatic potential. *J. Natl Cancer Inst.*, **80**, 200–204.
37. Leone,A., Flatow,U., VanHoutte,K. and Steeg,P.S. (1993). Transfection of human nm23-H1 into the human MDA-MB-435 breast carcinoma cell line: effects on tumor metastatic potential, colonization and enzymatic activity. *Oncogene*, **8**, 2325–2333.
38. Parhar,R.S., Shi,Y., Zou,M., Farid,N.R., Ernst,P. and Al-Sedairy,S. (1995) Effects of cytokine-mediated modulation of nm23 expression on the invasion and metastatic behavior of B16F10 melanoma cells. *Int. J. Cancer*, **60**, 204–210.
39. Baba,H., Urano,T. and Okada,K. (1995) Two isotypes of murine nm23/nucleoside diphosphate kinase, nm23-M1 and nm23-M2, are involved in metastatic suppression of a murine melanoma line. *Cancer Res.*, **55**, 1977–1981.
40. Freije,J.M.P., MacDonald,N.J. and Steeg,P.S. (1998) Nm23 and tumor metastasis: basic and translational advances. *Biochem. Soc. Symp.*, **63**, 261–271.
41. Lacombe,M., Milon,L., Munier,A. and Lambeth,D.O. (2000) The human Nm23/nucleoside diphosphate kinases. *J. Bioenerg. Biomembr.*, **32**, 247–258.
42. Parks,R.E.,Jr and Agarwal,R.P. (1973) Nucleoside diphosphokinases. In Boyer,P.D. (ed.), *The Enzymes*, 3rd Edn. Academic Press, New York, Vol. 8, pp. 307–333.
43. Wagner,P. and Vu,N.D. (1995) Phosphorylation of ATP-citrate lyase by nucleoside diphosphate kinase. *J. Biol. Chem.*, **270**, 21758–21764.
44. Engel,M., Veron,M., Theisinger,B., Lacombe,M.L., Seib,T., Dooley,S. and Welter,C. (1995) A novel serine/threonine-specific protein phosphotransferase activity on Nm23/nucleoside-diphosphate kinase. *Eur. J. Biochem.*, **234**, 200–207.
45. Wagner,P.D., Steeg,P.S. and Vu,N.D. (1997) Two-component kinase-like activity of nm23 correlates with its motility-suppressing activity. *Proc. Natl Acad. Sci. USA*, **94**, 9000–9005.
46. MacDonald,N.J., De la Rosa,A., Bebedict,M.A., Frejie,J.M.P., Krutsch,H. and Steeg,P.S. (1993) A serine phosphorylation of Nm23, and not its nucleoside diphosphate kinase activity, correlates with suppression of tumor metastatic potential. *J. Biol. Chem.*, **268**, 25780–25789.
47. Hemmerich,S. and Pecht,I. (1992) A cromoglycate binding protein from rat mast cells of a leukemia line is a nucleoside diphosphate kinase. *Biochemistry*, **31**, 4580–4587.
48. Lombardi,D., Sacchi,A., D'Angostino,G. and Tibursi,G. (1995) The association of the Nm23-M1 protein and β-tubulin correlates with cell differentiation. *Exp. Cell Res.*, **217**, 267–271.
49. Biggs,J., Hersperger,E., Steeg,P.S., Liotta,L.A. and Shearn,A. (1990) A *Drosophila* gene that is homologous to a mammalian gene associated with tumor metastasis codes for a nucleoside diphosphate kinase. *Cell*, **63**, 933–940.
50. Roymans,D., Vissenberg,K., De Jongle,C., Willems,R., Engler,G., Kiruma,N., Brobben,B., Claes,P., Verbelen,J.-P., Van Broeckhoven,C. *et al.* (2001) Identification of the tumor metastasis suppressor Nm23-H1/Nm23-R1 as a constituent of the centrosome. *Exp. Cell Res.*, **262**, 145–153.
51. Hannon,G.J., Demetrick,D. and Beach,D. (1993) Isolation of the Rb-related p130 through its interaction with CDK2 and cyclins. *Genes Dev.*, **7**, 2378–2391.
52. Wang,J., Xie,L.Y., Allan,S., Beach,D. and Hannon,G.J. (1998) Myc activates telomerase. *Genes Dev.*, **12**, 1769–1774.
53. Guan,K.L. and Dixon,J.E. (1991) Eukaryotic proteins expressed in *E.coli*: an improved thrombin cleavage and purification procedure of fusion proteins with glutathione S-transferase. *Anal. Biochem.*, **192**, 262–267.
54. Du,J., Nasir,I., Benton,B.K., Kladde,M.P. and Laurent,B.C. (1998) Sth1p, a *Saccharomyces cerevisiae* Snf2p/Swi2p homolog, is an essential

ATPase in RSC and differs from Snf/Swi in its interactions with histones and chromatin-associated proteins. *Genetics*, **150**, 987–1005.
55. Xiong,Y., Zhang,H. and Beach,D. (1993) Subunit rearrangement of the cyclin-dependent kinases is associated with cellular transformation. *Genes Dev.*, **7**, 1572–1583.
56. Vorobjev,I.A., Uzbekov,R.E., Komarova,Yu.A. and Alieva,I.B. (2000) Gamma-tubulin distribution in interphase and mitotic cells upon stabilization and depolymerization of microtubules. *Membr. Cell Biol.*, **14**, 219–235.
57. Giet,R. and Prigent,C. (2001) The non-catalytic domain of the *Xenopus laevis* aurora-A kinase localizes the protein to the centrosome. *J. Cell Sci.*, **114**, 2095–2104.
58. Biggs,J., Hersperger,E., Steeg,P.S., Ioitta,L.A. and Shearn,A. (1990) A *Drosophila* gene that is homologous to a mammalian gene associated with tumor metastasis codes for a nucleoside diphosphate kinase. *Cell*, **63**, 933–940.

Suppression of p160ROCK bypasses cell cycle arrest after Aurora-A/STK15 depletion

Jian Du and Gregory J. Hannon*

Cold Spring Harbor Laboratory, 1 Bungtown Road, Cold Spring Harbor, NY 11724

Edited by Stephen J. Elledge, Harvard Medical School, Boston, MA, and approved April 30, 2004 (received for review December 19, 2003)

Alterations in the expression and activity of the centrosomal kinase, Aurora-A/serine/threonine kinase 15 (STK15), affect genomic stability, disrupt the fidelity of centrosome duplication, and induce cellular transformation. Here, we provide evidence that p160ROCK, a Rho-associate serine/threonine kinase, associates with Aurora-A in a protein complex with other STK15-associated factors. Suppression of Aurora-A by small interfering RNA in HeLa cells blocks the ability of centrosomes to organize normal mitotic spindles, induces G_2/M cell cycle arrest, and promotes accumulation of tetraploid cells. In many cases, one outcome of such abnormalities is apoptosis. Introduction of a second genetic lesion, suppression of p160ROCK by RNA interference, can rescue abnormal mitotic spindle formation, release the G_2/M cell cycle arrest, and alleviate apoptosis, leading to a greater accumulation of aneuploid cells. These results suggest that Aurora-A and p160ROCK act in a common genetic pathway that promotes and monitors progression through G_2/M.

The eukaryotic centrosome is the microtubule-organizing center and is composed of two perpendicularly positioned centrioles and surrounding amorphous pericentriolar materials (for reviews, see refs. 1–6). Four groups of protein kinases are found to regulate the centrosome replication cycle: cyclin-dependent kinases (7–9), Polo-like kinases (10), NIMA kinases (11), and Aurora kinases. In mammalian cells, the Aurora kinase family has three members: Aurora-A, -B, and -C. Alterations in the expression and activity of Aurora-A/serine/threonine kinase 15 (STK15) affect genomic stability, disrupt the fidelity of centrosome duplication, and induce cellular transformation (12–15). Aurora-A is regulated by ubiquitin pathways and protein phosphorylation (16–19). A kinesin-related protein (Eg5), cytoplasmic polyadenylation element-binding protein (CPEB), and transforming acidic coiled-coil protein number 3 (TACC3) have been found to be substrates of Aurora-A (20–23).

Recently, p160ROCK has been identified as a centrosome component and functions in centrosome positioning and centrosome-dependent exit from mitosis (24). p160ROCK is a member of Rho-associated serine-threonine protein kinases. p160ROCK/Rho-kinase/ROK kinases are involved in various cellular functions downstream of Rho, such as smooth muscle contraction, stress fiber formation, and cytokinesis (25). p160ROCK phosphorylates LIM kinase and mDia, which then phosphorylates cofilin to regulate the Rho-induced reorganization of cytoskeleton (26). p160ROCK has also been reported to interact with CDC25A in transforming growth factor β-induced cell cycle arrest (27) and to be involved in tumorigenesis (28, 29), and apoptosis (30). Here we provide biochemical and genetic evidence that Aurora-A and p160ROCK associate physically and functionally in a protein complex. These proteins interact genetically, with suppression of p160ROCK alleviating the G_2/M cell cycle arrest induced by inactivation of Aurora-A.

Materials and Methods

Cell Culture. Normal human foreskin fibroblast IMR90 cells were immortalized by hTERT expression, and early passage HeLa and LinXA (293Tt derivative as in ref. 31) were cultured as in ref. 32. To assess mitotic spindle reassembly capacity *in vivo*, microtubules were disassembled with nocodazole and cold treatment (32). The cells were incubated at 37°C for 10 min to promote spindle reassembly. This process was monitored by anti-β-tubulin indirect immunofluorescence. p160ROCK specific inhibitor Y27632 (Calbiochem) was used at 100 μM in Fig. 2*b*.

Antibodies. Affinity-purified anti-Aurora-A, anti-GST-Aurora-A sera (32), rabbit polyclonal anti-γ-tubulin, mouse monoclonal anti-α-tubulin, anti-β-tubulin (Sigma), rabbit anti-phospho-H3 (Ser-10, Upstate Biotechnology, Lake Placid, NY), mouse monoclonal anti-BrdUrd (Amersham Pharmacia), rabbit polyclonal anti-MAD2 (Covance, Berkeley, CA), anti-p160ROCK serum (a kind gift from Shuh Narumiya, Kyoto University, Kyoto), anti-BubR1 and anti-Bub1 (kind gifts from S. Taylor, Manchester, U.K.), anti-DDX3 and DDX6 (kind gifts from J. Sommerville, University of St. Andrews, St. Andrews, Scotland and A. H. Patel, Medical Research Council, Institute of Virology, Glasgow, U.K.) were used. Another rabbit polyclonal anti-p160ROCK antibody against the C-terminal 9 aa (VKNTSGKTS) of p160ROCK was affinity-purified as in ref. 32.

Immunoprecipitation, Immunofluorescence, Immunoblot, and Aurora-A Depletion Assay. Immunoprecipitation, immunofluorescence, and immunoblotting were as described in ref. 32. Denaturing immunoprecipitation was done as in ref. 33. To measure how much p160ROCK associates with Aurora-A *in vivo*, we used increasing amounts of anti-GST-Aurora-A serum, and found that Aurora-A in 1×10^6 immortalized IMR90 cells can be 90% depleted by using 50 μl of anti-GST-Aurora-A serum. In Fig. 1*c*, the same amount of anti-Aurora-A antibody was used and images on immunoblot were captured with Alphaimager 2200 and quantified by CHEMILMAGER V5.5 program (Alpha Innotech, San Leandro, CA).

^{35}S-Labeling of Cells. IMR90 or cancer cell lines (2×10^6 cells) were labeled with ^{35}S-translabeling mixtures (Easy tag express [^{35}S] protein-labeling mix, 1,175 Ci/mmol; NEN) for 4 h. The cells were lysed, and immunoprecipitations were as in ref. 32.

Peptide Sequencing, MS Analysis, and Sequence Identification. Preparative immunoprecipitates from 2.5×10^8 IMR90 cells by using 1.5 mg of affinity-purified anti-Aurora-A antibody were resolved in 10% or 12% SDS-polyacrylamide gel and stained by Bio-Safe Coomassie G250 (Bio-Rad) or sequencing-grade Coomassie blue G250 (Sigma). Individual bands were excised and digested with trypsin, and peptides were fractionated by RP-HPLC. The MS sequencing was done in the Bio-medical Mass Spectrometry Facility at Washington University, St. Louis, as in ref. 34.

This paper was submitted directly (Track II) to the PNAS office.

Abbreviations: STK15, serine/threonine kinase 15; SAF, STK15-associate factor; RNAi, RNA interference; siRNA, small interfering RNA.

*To whom correspondence should be addressed. E-mail: hannon@cshl.edu.

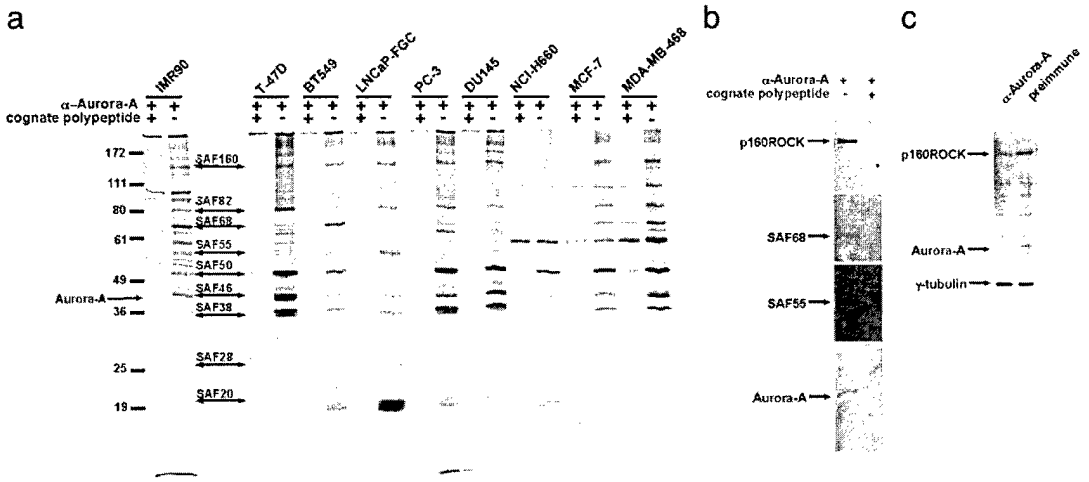

Fig. 1. Aurora-A and p160ROCK associate in a protein complex. (*a*) IMR90 cells, several prostate (LNCaP-FGC, PC-3, DU145, and NCI-H660), and breast (T-47D, BT549, MCF-7, and MDA-MB-468) cancer cell lines were labeled with [^{35}S]methionine. Cell lysates were immunoprecipitated with affinity-purified anti-Aurora-A antibody (αAurora-A+ lanes) or anti-Aurora-A plus cognate antigen polypeptide (αAurora-A+/cognate polypeptide+ lanes) and were resolved on SDS-10% polyacrylamide gel and subjected to autoradiography. SAFs with numbers indicate the apparent molecular mass on the gel, starting from the largest component (160 kDa). Molecular mass markers are indicated on the left. (*b*) Anti-p160ROCK, -SAF68, -SAF55, and -Aurora-A immunoblotting on anti-Aurora-A immunoprecipitates from IMR90 cells. (*c*) IMR90 cell lysates that were either titrated with anti-GST-Aurora-A to remove Aurora-A protein, or with same amount of preimmune sera as a control were subjected to immunoblotting with anti-p160ROCK and Aurora-A. Tubulin was used as a loading control.

RNA Interference (RNAi) in Transient Transfection. To design target-specific small interfering RNA (siRNA) duplexes, AA(N19)dTdT type sequences were selected from the ORFs of the p160ROCK (AAGGTGATTGGTAGAGGTGCA), Aurora-A (AAGCA-CAAAAGCTTGTCTCCA), and GFP (TCAGCGTGTCCGGC-GAGGGCGA) (35). The selected sequences were submitted to BLAST searches against the nonredundant protein database in National Center for Biotechnology Information to make sure that only the selected genes were targeted. The 21-nt RNAs purchased form Dharmacon (Lafayette, CO). In brief, 100 nM siRNA was used with transfection reagent Oligotransfectamine (Invitrogen) in HeLa cell transfections as in ref. 35. The 24-, 48-, and 72-h time points had one, two, and three rounds of transfections, respectively. Cells were assayed 24 h after the last transfection.

Flow Cytometry. Transfected HeLa cells were trypsinized and fixed for flow cytometry on Becton Dickinson FACSCalibur or LSRII as in ref. 36. The data were processed for cell cycle distribution by MODFIT V.2 (Macintosh) or V.3 (PC).

Apoptosis Assay. HeLa cells transfected in six-well cell-culture plates were trypsinized. The cells together with the culture media were spun down at 1,000 rpm in a tabletop centrifuge, and cells were stained with Hoechst 33342 to visualize the nuclei DNA morphology. Cells with intact uniform nuclei were counted as live cells and cells with fragmented nuclei, a signature of apoptosis cell, were counted as apoptotic cells (37). Annexin V-FITC apoptosis detection kit II (BD Pharmingen) and terminal deoxynucleotidyltransferase-mediated dUTP nick end-labeling assay (*In Situ* cell death detection kit, Roche Applied Science) were used according to the manufacturers' instructions.

Results and Discussions

To identify regulators and substrates of Aurora-A kinase, immortalized human IMR90 fibroblast cells were labeled with ^{35}S and Aurora-A was immunoprecipitated from cell lysates with affinity purified polyclonal anti-Aurora-A antibodies. Nine protein bands associated specifically with the antibody (Fig. 1*a*). We named the immunoprecipitated Aurora-A-bound protein STK15-associate factors (SAFs; see below).

The integrity of STK15 complexes is compromised in various breast and prostate cancer cell lines tested. However, SAF160 appears in every cell line examined, pointing to the potential importance of its association with Aurora-A (Fig. 1*a*). To identify components of the Aurora-A complex, Aurora-A-associated protein bands were excised and analyzed by matrix-assisted laser desorption ionization–time-of-flight MS and electrospray ionization MS/MS. Mass fingerprinting indicated that the 46-kDa protein was Aurora-A and that SAF160 was p160ROCK. Immunoblotting Aurora-A immunoprecipitates showed that anti-Aurora-A specifically immunoprecipitated Aurora-A, and p160ROCK, SAF68, and SAF55 (also identified as DDX3 and DDX6 by matrix-assisted laser desorption ionization–time-of-flight) (Fig. 1*b*). Immunoblot analysis demonstrated that γ-tubulin is not present at detectable levels in the SAF immunocomplex (data not shown). Therefore, it is unlikely that the purified SAF complex represents part of the centrosome that is indirectly associated with Aurora-A through γ-tubulin. TPX2 has been found to interact with Aurora-A by immunoprecipitation (38). However, we did not see a band of 100 kDa corresponding to TPX2 (Fig. 1*a*). Use of different anti-Aurora-A antibodies, cell lines, and labeling methods may account for this discrepancy in the immunoprecipitation results.

To examine whether SAFs coexist with Aurora-A in a large multiprotein complex, IMR90 lysates were fractionated by FPLC. All the identified proteins cofractionated with Aurora-A on Mono S and Mono Q ion-exchange columns and on a third Superose 6 gel filtration column (Fig. 5*a*, which is supporting information on the PNAS web site). On Superose 6, Aurora-A split into two distinct peaks, indicating that Aurora-A exists in multiple protein complexes (Fig. 5*b* and ref. 32). Immunodepletion with anti-GST-Aurora-A antibody in IMR90 cell lysates suggested that roughly half of endogenous p160ROCK associates with Aurora-A (Fig. 1*c*), either at the centrosome or in the cytoplasm (24).

We used RNAi to investigate consequences of suppressing Aurora-A or p160ROCK in HeLa cells. siRNAs dramatically reduced the expression of targeted proteins (Fig. 2*a*). Immunofluorescence stains with anti-Aurora-A and -p160ROCK also confirmed the depletions. The depletion of Aurora-A also

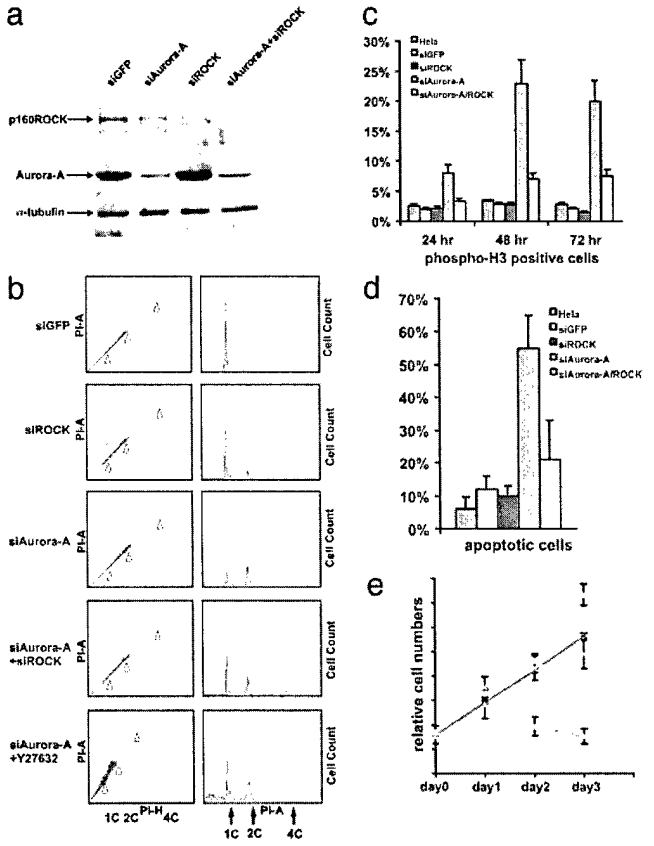

Fig. 2. Depletion of Aurora-A in HeLa cells induces G_2/M cell cycle arrest and apoptosis, but further deletion of p160ROCK alleviates this phenotype. HeLa cells with siGFP, siAurora-A, siROCK, or both, were used at 48 h after transfection. (*a*) Cell lysates (25 μg) were subjected to immunoblot assay by anti-Aurora-A, -p160ROCK, and -tubulin. The proteins are indicated on the left. (*b*) Cells treated with various siRNAs and/or Y-27632 were collected, fixed, and analyzed by flow cytometry. The blue portion indicates the diploid cells. The red portion indicates apoptotic cells, and the green portion indicates tetraploid/aneuploid cells. 1C, 2C, and 4C DNA contents are also indicated by arrows. (c, complete haploid DNA content). (*c*) Cells were stained for mitotic marker by using anti-phospho-H3 antibody, counterstained by Hoechst 33342 to visualize nuclei, and subjected to immunofluorescence microscopy. (*d*) Cells were collected including the floating cells in the media. Precipitated cells were resuspended in mounting media supplemented with Hoechst 33342 to stain DNA in the nuclei, and checked under a microscope for apoptotic cells. (*e*) HeLa cells were plated in six-well plates and transfected with siRNAs. At the indicated time, cells were collected and counted. Purple line, siGFP; yellow line, siROCK; green line, siAurora-A; blue line, siAurora-A+siROCK. In *c–e*, three independent experiments were performed and in each experiment, >300 cells were counted. Error bars are labeled on the top.

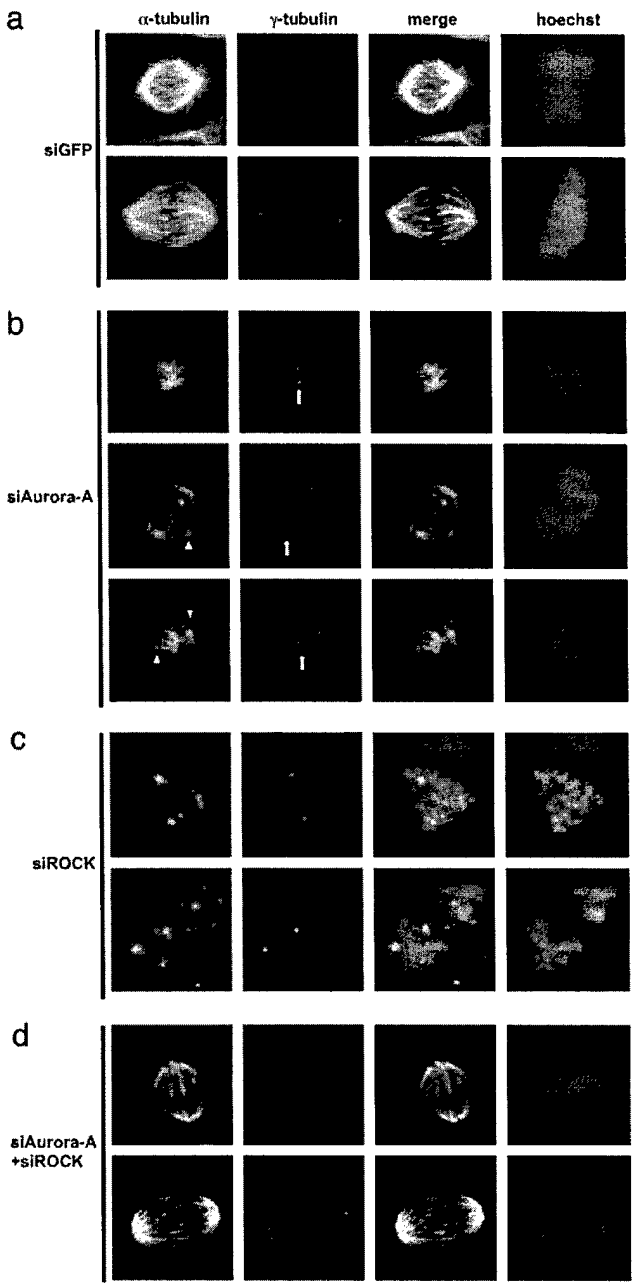

Fig. 3. Depletion of Aurora-A in HeLa cells causes abnormal mitotic spindles and split centrosomes in mitotic arrested cells, but further deletion of p160ROCK alleviates the phenotype. HeLa cells transfected with siGFP (*a*), siAurora-A (*b*), siROCK (*c*), or both (*d*) were subjected to immunofluorescence analysis with anti-α-tubulin to visualize mitotic spindles, anti-γ-tubulin to visualize centrosomes, and Hoechst 33342 to visualize nuclei DNA morphologies. The merge lane combines the anti-α- or anti-γ-tubulin images together for colocalization. In c cells were treated with nocodazole and cold to dissipate the microtubule networks. The mitotic spindles were allowed to reassemble for 10 min in 37°C.

significantly reduced the p160ROCK protein level (Fig. 2*a*), consistent with the notion that two proteins interact in a complex *in vivo* (39).

Twenty-four hours after transfection of siAurora-A, cells became rounder and grew more slowly than the control siGFP-transfected cells. Flow cytometry showed a significant increase in G_2/M phase cells in comparison with that observed in the control siGFP- or siROCK-treated cells (Fig. 2*b Right*). Notably, this cell cycle phenotype could be alleviated by simultaneous cotransfection of siRNAs directed against Aurora-A and p160ROCK (Fig. 2*b Right*, siAurora-A+siROCK). Correspondingly, a ROCK kinase specific inhibitor, Y27632, also showed a dosage-dependent suppression of the G_2/M arrest phenotype in siAurora-A-transfected cells (Fig. 2*b Right*, siAurora-A+Y27632). These results demonstrate an epistatic relationship between Aurora-A and p160ROCK and indicate that they function in the same genetic pathway.

The observed phenotypes were also confirmed by immunofluorescence staining of cells with anti-phospho-H3 antibody, a mitotic marker that specifically labels cells from the beginning of prophase to the end of anaphase (Fig. 2*c*). Quantitation of anti-phospho-H3 staining by flow cytometry supported interpretations from the immunofluorescence studies (data not

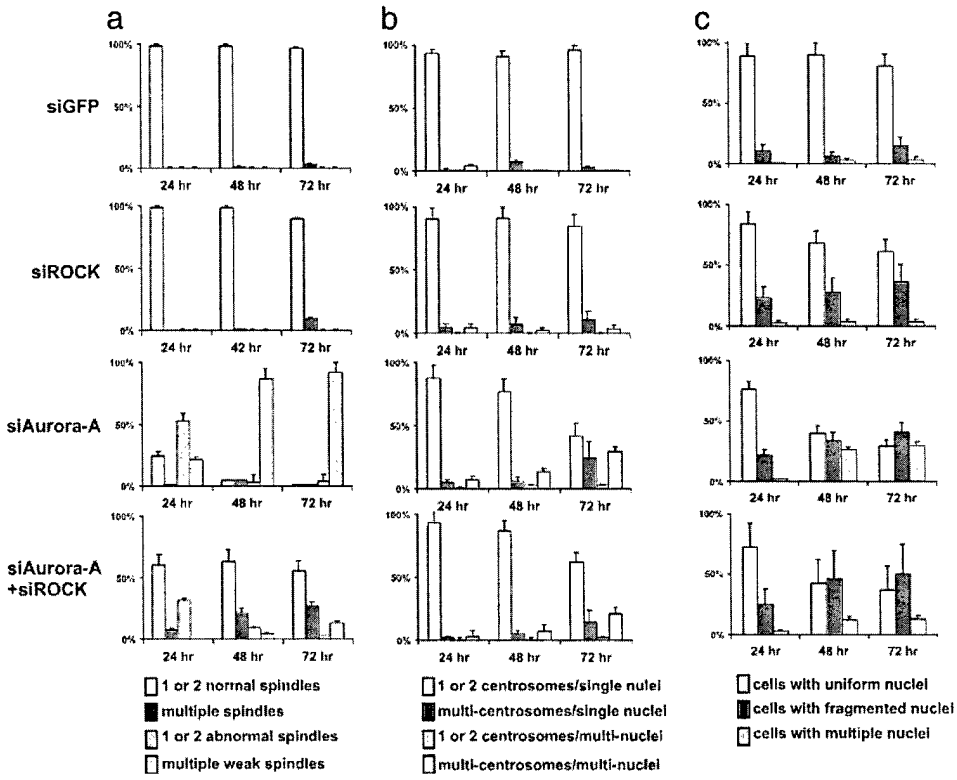

Fig. 4. Depletion of Aurora-A, p160ROCK, or both induces genomic instability. HeLa cells were analyzed 24, 48, and 72 h after transfection with siRNAs for mitotic spindle (*a*), centrosome (*b*), and nuclear (*c*) morphologies. (*a*) Spindles that can organize arrays of extended microtubules were counted as normal, either with one or two spindles, or with multiple (>2) spindles. Disorganized, distinctively fewer, and shorter spindles were counted as weak spindles (either one or two, or multiple). (*b*) Centrosomes were grouped according to their numbers in either single or multiply (≥2) nucleated cells. (*c*) Nuclei with free chromosome(s) (satellite nuclei), lagging chromosomes between two cells, string-like (abnormal chromosomes that were fragmented or unraveled), misplaced (positions in the cells dramatically deviated form wild-type controls), were counted as fragmented nuclei. The nuclei with perfectly round, smooth edges were counted as uniform nuclei. Cells with more than two nuclei were counted as cells with multiple nuclei. Three independent experiments were conducted and in each experiment, at least 100 mitotic (*a*) or 200 (*b* and *c*) cells were examined.

shown). BrdUrd incorporation to assess the S-phase population did not show a noticeable difference in the transfected cells at any time point (data not shown). The significantly prolonged mitotic phase correlated with an increased frequency of apoptosis (Fig. 2*d*), which was also confirmed by annexin V staining and terminal deoxynucleotidyltransferase-mediated dUTP nick end-labeling assays (data not shown) and a decrease in surviving cell numbers as measured by plotting growth curves (Fig. 2*e*). Again, cotransfection of siROCK together with siAurora-A partially rescued the apoptotic phenotype (Fig. 2 *d* and *e*).

Because Aurora-A is a centrosomal kinase, we next assessed the integrity of mitotic spindles and examined centrosome and nuclear morphologies in siAurora-A-transfected cells (Fig. 3). Most mitotic cells contained abnormal spindles with disorganized arrays of microtubules and fewer and shorter spindles than in normal control cells (Fig. 3*b*, anti-α-tubulin columns in siAurora-A images). In addition, comparison of the spindle lengths, intensities, and levels of the anti-α-tubulin stains in siAurora-A-treated cells with those of siGFP control cells showed that the spindle microtubule networks in Aurora-A-depleted cells did not extend to the condensed prometaphase chromosomes (Fig. 3 *a* and *b*, anti-α-tubulin columns). Some of the abnormal spindles still apparently radiated from centrosomes (Fig. 3*b*). Others had multiple origins that did not always colocalize with centrosomes or concentrations of γ-tubulin (Fig. 3*b*, anti-α-tubulin stains indicated by triangles). The portion of cells with abnormal spindles increased dramatically over the time course of the experiment (Fig. 4*a*). This outcome is the most prominent defect in the siAurora-A-transfected cells. Anti-γ-tubulin staining showed that with abnormal mitotic spindles, multiple concentrated spots of γ-tubulin occurred in the cytoplasm (Fig. 3*b*, anti-γ-tubulin spots indicated with arrows). Suppression of Aurora-A also induced centrosome amplification in interphase cells (Fig. 4*b*). Although chromosomes condensed at prometaphase in arrested mitotic cells, virtually no normal metaphase and anaphase mitotic figures were found in these transfected cells, suggesting cells arrested at prometaphase (Fig. 3*b*). Live cell imaging over a 4-h time course showed no progression of the arrested cells to metaphase, whereas control cells progressed from prometaphase through anaphase in ≈50 min (data not shown). siRNAs to Aurora-A also resulted in a significant accumulation of binucleated cells (Fig. 4*c*). Many nuclei had satellite micronuclei around the major interphase nucleus. In addition, many nuclei showed irregular undefined edges and shapes, a phenotype that often accompanies genomic instability and aneuploidy. The cell population with these unusual nuclear morphologies increased dramatically over the time course of the experiment (Figs. siAurora-A, 4C portion 2*b Left*, and 4*c*), indicating an increase in genomic instability of the cells. The mitotic spindle defects we observed here are closely resemble to those recently observed in Aurora-A-depleted HeLa cells (38, 40).

In siROCK-transfected cells, the number of cells with multiple mitotic spindles and the number of cells with apparent centrosome amplification in interphase cells increased significantly in comparison with siGFP control cells (Fig. 4 *a* and *b*). A dramatic

increase in mitotic spindle reassembly capacity was also observed in siROCK-transfected cells (see *Materials and Methods*). Eighty percent of mitotic cells showed multiple, reassembled mitotic spindle networks after transient treatment with nocodazole (Fig. 3*c*, anti-α-tubulin columns in siROCK images), in comparison with 20% of control cells. The result showed the siROCK-transfected cells are highly prone to reassembling inappropriate mitotic spindles using nascent γ-tubulin spots. In accordance with this result, we observed an increase in aneuploid cells (Figs. siROCK, 4C portion 2*b Left*, and 4*c*). Also, siROCK transfection caused nuclear fragmentation (Fig. 4*c*). However, a dramatic increase did not occur in multinucleated cell populations (Fig. 4*c*). This result suggests that depletion of p160ROCK alone can give rise to aneuploid cells, although to a lesser degree than does loss of Aurora-A.

Again, we found the mitotic arrest caused by suppression of Aurora-A was alleviated by coincident depletion of p160ROCK (Fig. 2 *b Right*, siAurora-A+siROCK, and *c*). Cotransfection of both siAurora-A and siROCK led to assemble of functional mitotic spindles (Fig. 3*d*, anti-α-tubulin columns in siAurora-A+siROCK images), completion of mitosis, regrouping of split centrosomes into two functional groups for organizing bipolar spindles (Fig. 3*d*, anti-γ-tubulin columns in siAurora-A+siROCK images), and greater accumulation of aneuploid cells (Figs. siAurora-A+siROCK, 4C portion 2*b Left*, and 4*c*).

The immunoprecipitated Aurora-A not only phosphorylated an artificial substrate, myelin basic protein, but also phosphorylated a p160 in the SAF complex (Fig. 6 *a* and *b*, which is published as supporting information on the PNAS web site). This finding was confirmed by denaturing IP to be p160ROCK (Fig. 6*c*). Aurora-A also phosphorylated another protein, p82, in purified centrosomes (Fig. 6 *a* and *b*). Phosphorylation of p160ROCK in the immunoprecipitated Aurora-A complex can be specifically increased in cells transfected with constructs encoding *Aurora-A*, but not a mutant *Aurora-A K162M*, which lacks kinase activity (41) (Fig. 6*d*). In fact, [^{32}P]orthophosphate labeling indicated that phosphorylation of p160ROCK in the cells expressing a kinase dead Aurora-A K162M mutant appreciably decreased, suggesting that Aurora-A is responsible, at least in part, for p160ROCK phosphorylation *in vivo* (Fig. 6*e*, comparing P-p160ROCK band intensity in K162M lane with those in other control lanes). Phosphoamino acid analysis of excised ^{32}P-labeled p160ROCK band showed that only serine residue(s) are phosphorylated (Fig. 7*a*, which is published as supporting information on the PNAS web site). *In vitro* kinase assays with various GST-p160ROCK fusion proteins as substrates for Aurora-A (Fig. 7*b*, all fusion proteins started from N terminus of p160ROCK and ended at the indicated amino acids) showed GST-p160ROCK1034 was significantly labeled, but not GST-p160ROCK726 or other fusion proteins (Fig. 7*c*), suggesting the phosphorylated serine residues are located between 726 and 1,034 aa of p160ROCK.

A G_2/M delay phenotype had been reported after overexpression of Aurora-A in HeLa cells (42). A similar mitotic defect is also observed on *Aurora-A* loss-of-function in *Drosophila melanogaster* and in S_2 cells (ref. 43 and data not shown) and most recently in HeLa cells (40, 44). These results together with our observation indicate that balance of Aurora-A protein in the cell is critical and that either down- or up-regulation of its protein level will compromise its function and lead to mitotic defects. Suppression of aurora-A (aurora-1) in *Caenorhabditis elegans* by RNAi does not affect centrosome separation, but mitotic spindle formation (45), similar to what we observed here in HeLa cells. However, in *D. melanogaster* syncytial embryos, aurora mutations cause centrosome separation defects, which result in monopolar spindles and abnormal mitoses. The differences between these observed phenotypes could be due to cell type-specific functions of Aurora kinases. However, we favor the notion that different genetic lesions (e.g., point mutation versus nearly, but not complete suppression by RNAi versus null mutations) leads to different phenotypic outcomes. Although a causal relationship between phosphorylation of p160ROCK by Aurora-A and suppression of mitotic arrest has not been firmly established here, our results indicate that p160ROCK acts downstream of Aurora-A in a common genetic pathway and phosphorylation of p160ROCK by Aurora-A may mimic the depletion of p160ROCK to bypass the mitosis arrest caused by Aurora-A inactivation.

We thank M. and C. Crankshaw (Washington University, St. Louis) for their expert help on MS, D. Helfman for his insight on the Y27632 and p160ROCK experiments, S. Narumiya (Kyoto, Japan) for his kind gift of the p160ROCK plasmid and antibody, S. Taylor, J. Sommerville, and A. H. Patel for kind gifts of antibodies, M. Mayer (Cold Spring Harbor Laboratory) for the help with the phosphoamino acid assay, G. Nourjanova for help on 2D protein gel, S. Prasanth for advice on HeLa cell transfection, P. Bubulya for help in live cell imaging, M. McCurrach for advice in BrdUrd labeling, A. Denli and A. Caudy for their critical reading of the manuscript and helpful discussion, and J. Duffy in the graphic arts department and S. Hearn in the microscope core facility (Cold Spring Harbor Laboratory) for their help. J.D. is supported by Postdoctoral Fellowship DAMD17-02-1-0344 from the Department of Defense Breast Cancer Research Program. This work is also supported by National Institutes of Health Grant P01-CA13106 (to G.J.H.).

1. Zheng, Y., Jung, M. K. & Oakley, B. R. (1991) *Cell* **65,** 817–823.
2. Hinchcliffe, E. H. & Sluder, G. (2001) *Curr. Biol.* **11,** R698–R701.
3. Bornens, M. (2002) *Curr. Opin. Cell Biol.* **14,** 25–34.
4. Rieder, C. L., Faruki, S. & Khodjakov, A. (2001) *Trends Cell Biol.* **11,** 413–419.
5. Doxsey, S. (2001) *Nat. Rev. Mol. Cell Biol.* **2,** 688–698.
6. Stearns, T. (2001) *Cell* **105,** 417–420.
7. Hinchcliffe, E. H., Li, C., Thompson, E. A., Maller, J. L. & Sluder, G. (1999) *Science* **283,** 851–854.
8. Matsumoto, Y., Hayashi, K. & Nishida, E. (1999) *Curr. Biol.* **9,** 429–432.
9. Meraldi, P., Lukas, J., Fry, A., Bartek, J. & Nigg, E. A. (1999) *Nat. Cell Biol.* **1,** 88–93.
10. do Carmo Avides, M., Tavarest, A. & Glover, D. M. (2001) *Nat. Cell Biol.* **3,** 421–424.
11. Fry, A. M. (2002) *Oncogene* **21,** 6184–6194.
12. Zhou, H., Kuang, J., Zhong, L., Kuo, W., Grey, J., Sahin, A., Brinkley, B. & Sen, S. (1998) *Nat. Genet.* **20,** 189–193.
13. Tanaka, T., Kimura, M., Matsunaga, K., Fukada, D., Mori, H. & Okano, Y. (1999) *Cancer Res.* **59,** 2041–2044.
14. Miyoshi, Y., Iwao, K., Egawa, C. & Noguchi, S. (2001) *Int. J. Cancer* **92,** 370–373.
15. Sen, S., Zhou, H., Zhang, R. D., Yoon, D. S., Vakar-Lopez, F., Ito, S., Jiang, F., Jounston, D., Grossman, H. B., Ruifrok, A. C., *et al.* (2002) *J. Natl. Cancer. Inst.* **94,** 1320–1329.
16. Farruggio, D. C., Townsley, F. M. & Ruderman, J. V. (1999) *Proc. Natl. Acad. Sci. USA* **96,** 7306–7311.
17. Walter, A., Seghezzi, O., Korver, W., Sheung, J. & Lees, E. (2000) *Oncogene* **19,** 4906–4916.
18. Honda, K., Mihara, H., Kato, Y., Yamaguchi, A., Tanaka, H., Yasuda, H., Furukawa, K. & Urano, T. (2000) *Oncogene* **19,** 2812–2819.
19. Katayama, H., Zhou, H., Li, Q., Tatsuka, M. & Sen, S. (2001) *J. Biol. Chem.* **276,** 46219–46224.
20. Giet, R., Uzbekov, R., Cubizolles, F., Le Guellec, K. & Prigent, C. (1999) *Biol. Cell* **91,** 461–470.
21. Mendez, R., Hake, L. E., Andresson, T., Littlepage, L. E., Ruderman, J. V. & Richter, J. D. (2000) *Nature* **404,** 302–307.
22. Groisman, I., Huang, Y. S., Mendea, R., Cao, Q., Theurkauf, W. & Richter, J. D. (2000) *Cell* **103,** 435–447.
23. Giet, R., McLean, D., Descamps, S., Lee, M. J., Raff, J. W. & Prigent, C. (2002) *J. Cell. Biol.* **156,** 437–451.
24. Chevrier, V., Piel, M., Collomb, N., Saoudi, Y., Frank, R., Paintrand, M., Narumiya, S., Bornens, M. & Didier, J. (2001) *J. Cell. Biol.* **157,** 807–817.
25. Amano, M., Fukata, Y. & Kaibuchi, K. (2000) *Exp. Cell Res.* **261,** 44–51.
26. Maekawa, M., Ishizaki, T., Boku, S., Watanabe, N., Fujita, A., Iwamatsu, A., Obinata, T., Ohashi, K., Mizuno, K. & Narumiya, S. (1999) *Science* **285,** 895–898.

27. Bhowmick, N. A., Ghiassi, M., Aakre, M., Brown, K., Singh, V. & Moses, H. L. (2003) *Proc. Natl. Acad. Sci. USA* **100,** 15548–15553.
28. Watnick, R. S., Cheng, Y. N., Rangarajan, A., Ince, T. A. & Weinberg, R. A. (2003) *Cancer Cell* **3,** 199–200.
29. Sahai, E. I. T., Narumiya, S. & Treisman, R. (1999) *Curr. Biol.* **9,** 136–145.
30. Coleman, M. L., Sahai, E. A., Yeo, M., Bosch, M., Dewar, A. & Olson, M. F. (2001) *Nat. Cell Biol.* **3,** 339–345.
31. Hannon, G. J., Sun, P., Carnero, A., Xie, L. Y., Maestro, R., Conklin, D. S. & Beach, D. (1999) *Science* **283,** 1129–1130.
32. Du, J. & Hannon, G. (2002) *Nucleic Acids Res.* **30,** 5465–5475.
33. Herbst, A. & Tansey, W. P. (2000) *Mol. Biol. Rep.* **27,** 203–208.
34. Grant, G. A. & Crankshaw, M. W. (2003) *Methods Mol. Biol.* **211,** 247–268.
35. Elbashir, S. M., Harborth, J., Lendeckel, W., Yalcin, A., Weber, K. & Tuschl, T. (2001) *Nature* **411,** 494–498.
36. Du, J., Nasir, I., Benton, B. K., Kladde, M. P. & Laurent, B. C. (1998) *Genetics* **150,** 987–1005.
37. Lassus, P., Optiz-Araya, X. & Lazebnik, Y. (2002) *Science* **297,** 1352–1354.
38. Kufer, T. A., Sillje, H. H., Korner, R., Gruss, O. J., Meraldi, P. & Nigg, E. A. (2002) *J. Cell Biol.* **158,** 617–623.
39. Laurent, B. L. & Carlson, M. (1992) *Genes Dev.* **6,** 1707–1715.
40. Hirota, T., Kunitoku, N., Sasayama, T., Marumoto, T., Zhang, D., Nitta, M., Hatakeyama, K. & Saya, H. (2003) *Cell* **114,** 585–598.
41. Bischoff, J. R., Anderson, L., Zhu, Y., Mossie, K., Ng, L., Souza, B., Schryver, B., Flanagan, P., Chairvoyant, F., Ginther, C., *et al.* (1998) *EMBO. J.* **17,** 3052–3065.
42. Meraldi, P., Honda, R. & Nigg, E. A. (2002) *EMBO, J.* **21,** 483–492.
43. Glover, D. M., Leibowitz, M. H., McLean, D. A. & Parry, H. (1995) *Cell* **81,** 95–105.
44. Kunitoku, N., Sasayama, T., Marumoto, T., Zhang, D., Honda, S., Kobayashi, O., Hatakeyama, K., Ushio, Y. H. S. & Hirota, T. (2003) *Dev. Cell* **5,** 853–864.
45. Schumacher, J. M., Ashcroft, N., Donovan, P. J. & Golden, A. (1998) *Development (Cambridge, U.K.)* **125,** 4391–4402.

Du and Hannon *et al.* 10.1073/pnas.0308484101.

Supporting Information

Files in this Data Supplement:

Supporting Figure 5
Supporting Figure 6
Supporting Figure 7

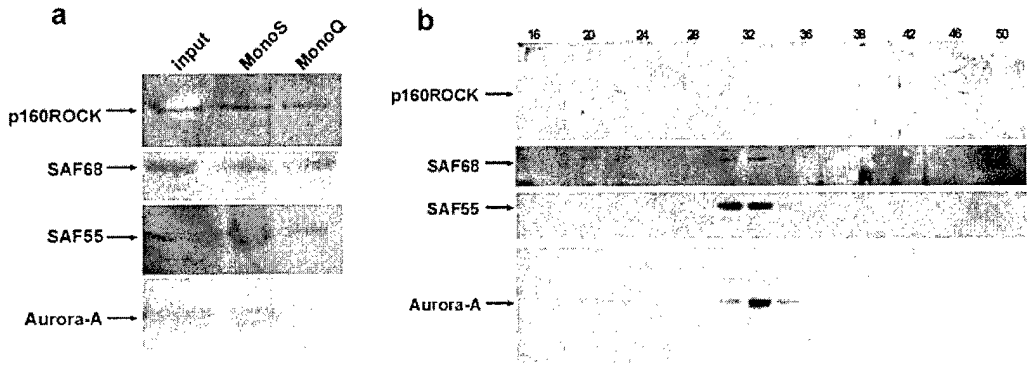

Fig. 5. STK15-associate factor (SAF) proteins coelute on FPLC. (*a*) p160ROCK, SAF68, SAF55, and Aurora-A cofractionate on MonoS and MonoQ ion-exchange columns. IMR90 cell lysates were applied to MonoS and then MonoQ columns. The Aurora-A fractions were followed and resolved on SDS-10% polyacrylamide gel, and tested for the presence of p160ROCK, SAF68, and SAF55. (*b*) Aurora-A fractions after MonoQ column were pooled and applied to Superose 6 column. Fractions 16-50 of 0.5 ml volume were collected and TCA-precipitated; every other fraction was loaded and resolved on SDS-10%

polyacrylamide gel for immunoblotting.

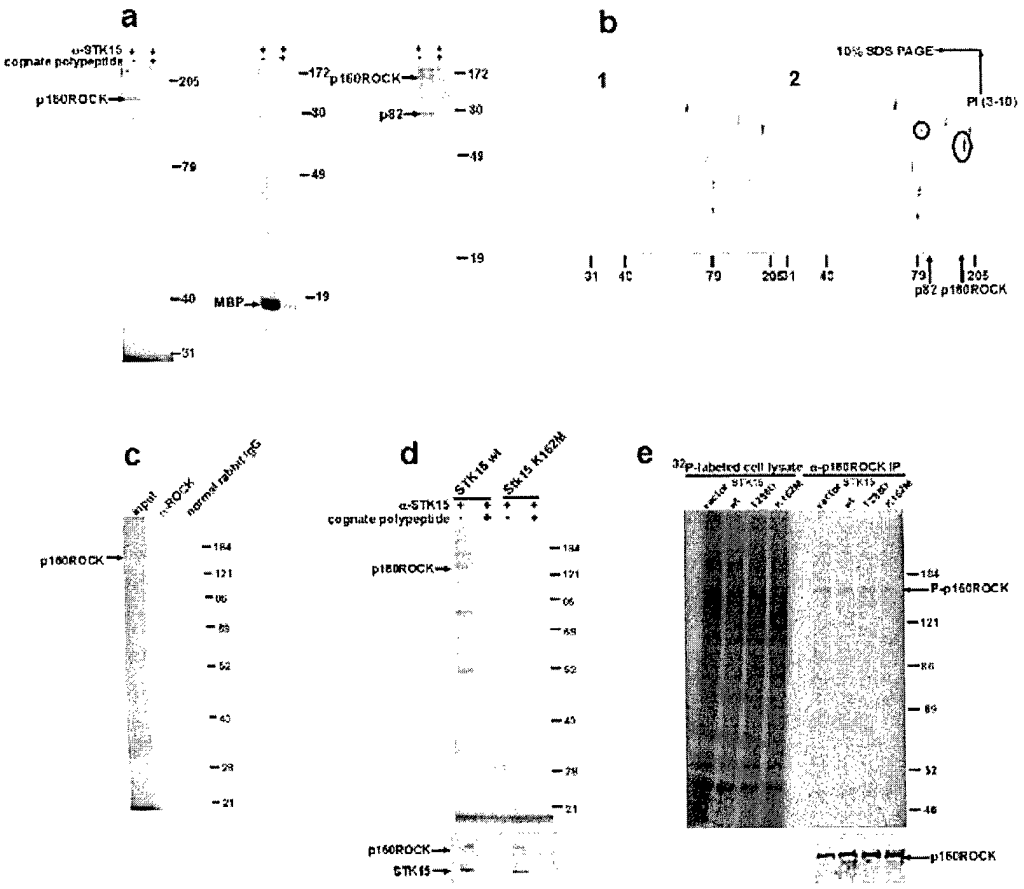

Fig. 6. p160ROCK is an Aurora-A kinase substrate *in vivo*. The protein bands are indicated on the left. The molecular mass markers are labeled on the right. (*a*) SAF complex immunoprecipitated from IMR90 cell lysates by affinity-purified anti-Aurora-A antibody without (a -Aurora-A+ lanes) or with cognate antigen polypeptide (cognate polypeptide+ lanes, controls) were subjected to kinase reactions (lanes 1 and 2), with artificial substrate myelin basic protein (MBP) (0.05 mg·ml^{-1} final concentration, lanes 3 and 4), or with purified centrosomes (2 m g, lanes 5 and 6). The kinase reactions using the immunoprecipitated Aurora-A (*b2*) or the mock immunoprecipitates (*b1*) were subjected to 2D electrophoresis and autoradiography. Phosphorylated SAF160 and p82 are indicated with cycles. (*c*) Kinase reactions from immunoprecipitated Aurora-A complex were

denatured and further immunoprecipitated with anti-p160ROCK antibody. Same amount of normal rabbit IgG was used as a control. Labeled p160ROCK can be immunoprecipitated specifically from the kinase reaction. (*d*) LinXA cells were transfected with *Aurora-A* wt, *Aurora-A K162M* constructs in pMaohygro vector. The precipitated proteins by a -Aurora-A from the cell lysates were subjected to kinase assay and resolved on SDS-10% polyacrylamide gel for autoradiography. p160ROCK can only be significantly phosphorylated from the *Aurora-A* wt transfected cells, but not from Aurora-A kinase-dead mutation *K162M.* The same immunoprecipitates were also subjected to immunoblotting for p160ROCK and Aurora-A to determine that same amount of proteins were precipitated from both samples. (*e*) LinXA cells transfected with vector alone, *Aurora-A wt*, *Aurora-AK162M*, and *Aurora-AT288D* constructs in pMaohygro vector. Cell lysates from ^{32}P labeling were immunoprecipitated using anti-p160ROCK antibody and bounded materials (lanes 5-8), and 5 m g of cell lysates from each transfected cells (lanes 1-4) were resolved on SDS-10% polyacrylamide gel and subjected to autoradiography. Immunoblotting showed that same amount of p160ROCK can be immunoprecipitated from the cell lysates of the transfections above.

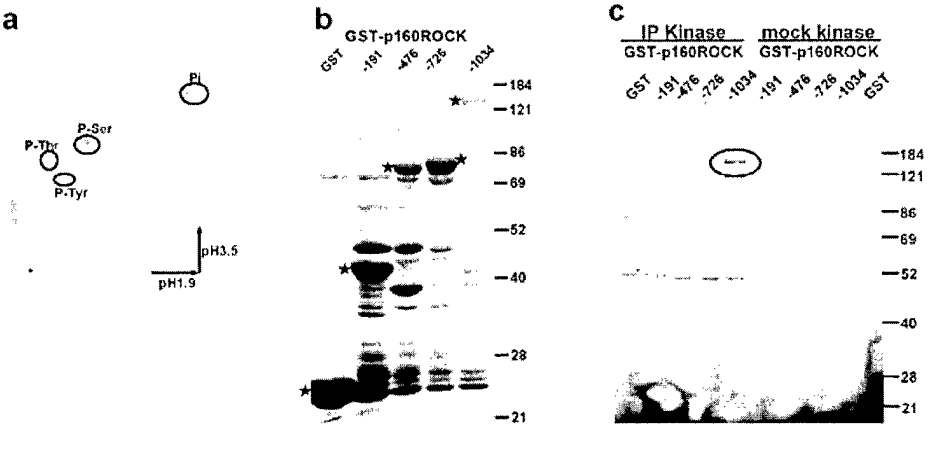

Fig. 7. Only serine residue(s) at C terminus of p160ROCK are phosphorylated by STK15. (*a*)

The p160ROCK band from kinase reactions with SAF complex from IMR90 cells was excised and subjected to phosphoamino acids assay. P-Ser, phosphoserine; P-Thr, phosphothreonine; P-Tyr, phosphotyrosine; Pi, phosphate. The origin is labeled with +. Only P-Ser showed significant signal. (*b*) GST-p160ROCK proteins were purified by using glutathione-agarose beads, resolved on SDS-10% polyacrylamide gel, and stained with Coomassie blue G-250. The fusion proteins on the gel are indicated with stars. (*c*) Ten micrograms of GST-p160ROCK fusion proteins were subjected to kinase assay with immunoprecipitated Aurora-A SAF complex from IMR90 with (mock kinase assay) or without (IP kinase assay) cognate polypeptide antigens. The only protein band (GST-p160ROCK1034) with significant ^{32}P labeling for phosphorylation is indicated with a circle. Molecular weight markers are indicated on the right.